2022-2024 RUQAYA KHURSHID SU92-MSCHW-F22-043 FOS

A Computational Approach To Assess The Importance Of Indoleamine 2, 3-Dioxygenase (IDO) As A Cancer Biomarker



SUPERIOR UNIVERSITY

Thesis Submitted to

The Superior University Lahore

In Partial Fulfillment of the

Requirement for the Degree of

M.Phil. Chemistry

By

RUQAYA KHURSHID

Roll No. SU92-MSCHW-F22-043

Session: 2022-2024

Faculty of Sciences

A Computational Approach To Assess The Importance Of Indoleamine 2, 3-Dioxygenase (IDO) As A Cancer Biomarker

SUPERIOR UNIVERSITY

Thesis Submitted to

The Superior University Lahore

In Partial Fulfillment of the

Requirement for the Degree of

M.Phil. Chemistry

By

RUQAYA KHURSHID

Roll No. SU92-MSCHW-F22-043

Session: 2022-2024

Faculty of Sciences

Author's Declaration

I hereby state that my M.Phil. thesis titled **"A Computational approach to assess the importance of indolamine 2,3-dioxygenase (IDO) as a cancer biomarker"** is my work and has not been submitted previously by me for taking any degree from this University,

The Superior University, Lahore

or anywhere else in the country/world.

At any time if my statement is found to be incorrect even after my graduation, the university has the right to withdraw my M.Phil. degree.

Name of Student: Ruqaya Khurshid

Date: _____

Plagiarism Undertaking

I solemnly declare that research work presented in the thesis titled **"A Computational approach to assess the importance of indolamine 2,3-dioxygenase (IDO) as a cancer biomarker"** is solely my research work with no significant contribution from any other person. Small contribution/help wherever taken has been duly acknowledged and that complete thesis has been written by me.

I understand the zero-tolerance policy of the HEC and University,

The Superior University, Lahore

towards plagiarism. Therefore, I as author of the above-titled thesis declare that no portion of my thesis has been plagiarized and any material used as a reference is properly referred/cited. I undertake that if I am found guilty of any formal plagiarism in the above-titled thesis, even after awarding of M.Phil. degree, the University reserves the rights to withdraw/revoke my M.Phil. degree and that HEC and the University have the right to publish my name on the HEC/University website on which names of students are placed who submitted a plagiarized thesis.

Student/Author Signature: _____

Name: Ruqaya Khurshid

Research Completion Certificate

This is to certify that the thesis entitled **"A Computational approach to assess the importance of indolamine 2,3-dioxygenase (IDO) as a cancer biomarker"** submitted by **"Ruqaya Khurshid"** has been accepted towards the partial fulfillment of the requirement for M.Phil., **"Chemistry"**. The quality of the work contained in thisthesis is adequate for the award of degree.

Supervisor: Dr. Rabia Nawaz
Designation: Assistant Professor
Department of Biological Sciences
Signature: _____

Certificate of Approval

This is to certify that the research work presented in this thesis, titled **"A Computational approach to assess the importance of Indolamine 2,3-dioxygenase (IDO) as a cancer biomarker"** was conducted by **"Ruqaya Khurshid"** under the supervision of **"Dr. Rabia Nawaz".**

No part of this thesis has been submitted anywhere else for any other degree. This thesis is submitted to the Faculty of Sciences, The Superior University, Lahore in partial fulfillment of the requirements for the degree of Master of Philosophy in the field of "**Chemistry"** in Faculty of Sciences at The Superior University, Lahore.

Student Name: Ruqaya Khurshid Signature:_____

Examination Committee:

Session Chair: Dr. M. Mudassir Iqbal Signature:_____

a) External Examiner: Dr. Misbah Naz
   Assistant Professor of Chemistry
   Division of science and technology, University of Education, Lahore.

   Signature:_____

b) Internal Examiner: Dr. Fizza Naseem Signature:_____

c) Supervisor Name: Dr. Rabia Nawaz Signature:_____

d) Name of HOD: Prof. Dr. Uqba Mehmood Signature:_____

e) Name of Dean: Prof. Dr. M. Naveed Babur Signature:_____

f) Controller Examination: Dr. Muhammad Haris Signature:_____

Dedication

I am grateful to **Allah**, the Most Merciful and Compassionate, for providing me with the guidance, strength, and perseverance to complete this thesis. Without His blessings, I would not have been able to overcome the challenges that came my way. I thank Him for the opportunity to learn and grow, and for the countless blessings He has bestowed upon me throughout this journey. May He continue to guide me in all my endeavors and grant me success in both this life and the hereafter.

I express my gratitude to my loving and affectionate parents **(Mr. and Mrs. Khurshid Anwar Khokhar)** who remember me and supported me in all respects. Their best wishes and trust made me confident enough to achieve my results.

My **siblings, friends,** and my **research fellows** have been a source of inspiration and support. I am thankful for their support, encouragement, and motivation throughout my academic journey.

Last but not least, I want to dedicate this thesis to myself and want to thank me for believing in me. I want to thank me for doing all this hard work. I want to thank me for having no days off.

Acknowledgments

In the name of Allah, the most Gracious, the most Merciful.

I am extremely thankful to Almighty ‘Allah’ Who is the entire source of knowledge and wisdom endowed to mankind, for providing me with the acumen and vision to complete this endeavor.

I would like to express my profound gratitude to my supervisor for her wise counsel and encouraging attitude towards this study. I am extremely grateful to her for immensely facilitating me during my study period by ensuring the provision of favorable circumstances and conducive environment. This project would not have been possible without her support and expert guidance.

In the end, I would like to extend my deepest gratitude to my family members. Without their encouragement, I would not have been able to complete this endeavor.

Ruqaya Khurshid

Table Of Contents

	Page #
Author Declaration	II
Plagiarism Undertaking	III
Research Completion Certificate	IV
Certificate of Approval	V
Dedication	VI
Acknowledgements	VII
Table of Content	VIII
List of Tables	XI
List of Figures	XII
List of Abbreviations	XIV
ABSTRACT	XV
CHAPTER 1 INTRODUCTION	01
AIMS AND OBJECTIVES	03
CHAPTER 2 LITERATURE REVIEW	04
CHAPTER 3 METHODOLOGY	17
3.1: Investigation of mRNA expression levels of IDO1 across different cancers	17
3.1.1: IDO1 expression using GEPIA	17
3.1.2: IDO1 expression using UALCAN	17
3.1.3: IDO1 expression using GENT2	17
3.2: Analysis of differential expression of IDO1 in Liver Cancer versus healthy tissue	18
3.2.1: Differential expression of IDO1 in cholangiocarcinoma using UALCAN	18
3.2.2: Differential expression of IDO1 in LIHC using GEPIA2	18
3.2.3: Differential expression of IDO1 in LIHC using UALCAN	18
3.3: Clinicopathological analysis of IDO in LIHC	19
3.4: Association between IDO1 expression and prognosis in cancer patients	19
3.4.1: Association between IDO1 expression and probability of LIHC patients using GEPIA	19
3.4.1.1: Retrieved data on Overall survival	19
3.4.1.2: Retrieved data on Disease Free Survival (DFS)	20
3.4.2: Association between IDO1 expression and probability in LIHC patients	

through R2 platform 20
3.4.3: Overall survival data retrieved from OncoLnc server 21
3.5: Co-expression analysis of IDO in LIHC cancer 21
3.5.1: Retrieval of positively Correlated genes of IDO1 in LIHC by using UALCAN 21
3.5.2: Correlation analysis of IDO1 gene in LIHC by using UCSC Xena 21
3.5.3: Correlation analysis of IDO1 gene in LIHC by using GEPIA2 22
3.6: Enrichment analysis of IDO using Enrichr 23
3.7: Evaluation of IDO interaction network 23
3.7.1: Protein-protein interaction using STRING database 23
3.7.2: IDO interaction network using GeneMANIA 24
3.8: Network analysis of IDO using NetworkAnalyst 24
3.8.1: Transcription factor (TF) analysis 24
3.8.2: miRNA network analysis 24
3.9: Quantum chemical analysis of IDO1's active site using density functional theory DFT study 25
3.10: Molecular docking analysis 26
3.10.1: Retrieval of ligand from PUBCHEM 26
3.10.2: Autodocking using Pyrx 26
3.10.3: 2D and 3D visualization on BIOVIA discovery studio 26
3.11: Statistical analysis of gene expression and patient survival in LIHC 26
3.11.1: IDO gene expression data retrieval through GEO database 26
3.11.1.1: Evaluation of diagnostic value of IDO gene through ROC curve 27
3.11.2: Survival data retrieval through OncoLnc 27
3.11.2.1: Evaluation of prognostic value of IDO1 gene through ROC curve 28
CHAPTER 4 RESULTS 22
4.1. mRNA Expression Levels Of IDO1 Across Different Cancers 29
4.1.1. Analysis With GEPIA 30
4.1.2. Analysis With UALCAN 31
4.1.3. Analysis With GENT2 32
4.2. Comparison Of IDO1 Expression In Liver Cancer With Healthy Tissues 32
4.2.1. Evaluation Of Differential Expression Of IDO1 In Cholangiocarcinoma Using

UALCAN 32
4.2.2. Evaluation Of Differential Expression Of IDO1 In LIHC Using GEPIA2 33
4.2.3. Evaluation Of Differential Expression Of IDO1 In LIHC Using UALCAN 35
4.3. Expression Analysis Of IDO1 In Relation To Clinicopathological Parameters In LIHC 35
4.4. Correlation Analysis Between IDO1 Expression And Prognosis In Cancer Patients 39
4.4.1. Association Analysis Between IDO1 Expression And Probability Of LIHC Patients Using GEPIA2 39
4.4.1.1. Overall Survival Data Analysis Through GEPIA2 39
4.4.1.2. Disease-Free Survival Analysis Through GEPIA2 40
4.4.2. Association Between IDO1 Expression And Probability In LIHC Patients Through R2 Platform 41
4.4.3. Overall Survival Data Analysis Through OncoLnc Server 43
4.5. Co-Expression Analysis Of IDO1 In LIHC 44
4.5.1. Positively Correlated Genes With IDO Using UALCAN 44
4.5.2. Correlation Analysis Between IDO1 And HLA-DOB 50
4.5.3. Correlation Analysis Between IDO1 And HLA-DOB Using GEPIA2 46
4.6. Enrichment Analysis Of IDO1 48
4.7. Evaluation Of IDO1 Interaction Network 52
4.7.1. Protein-Protein Interaction Using STRING Database 52
4.7.2. IDO1 Interaction Network Using Genemania 53
4.8. Network Analysis Of IDO1 Using Network Analyst 54
4.8.1. Transcription Factor (TF) Analysis 54
4.8.2. miRNA Network Analysis Of IDO1 55
4.9: Quantum Analysis Of Active Site Of IDO1 Using Density Functional Theory DFT 56
4.10: Molecular Docking Of IDO1 With Ligand Quercetin 58
4.11. Statistical Analysis Of Gene Expression And Patient Survival In LIHC 60
4.11.1. Evaluation Of Diagnostic Value Of IDO1 60
4.11.2. Evaluation Of Prognostic Value Of IDO 60
CHAPTER 5 DISCUSSION 62
CHAPTER 6 CONCLUSION 70

REFERENCES 71
APPENDICES XVI
Appendix- 1 XVI

List Of Tables

Table No	Description	Page #
4.1	Positive correlated genes with IDO in LIHC	46
4.2	Top Enriched BioPlanet 2019 Pathways Identified via Enrich	49
4.3	Top Enriched KEGG Pathways 2021 Human Identified via Enrichr	49
4.4	Top Enriched Reactome Pathways 2024 Identified via Enrichr	50
4.5	Top Enriched WikiPathways 2024 Human Identified via Enrichr	50
4.6	Top Enriched Elsevier Pathways Identified via Enrichr	50
4.7	Top Enriched Biological Processes (GO-BP) 2025 for IDO1 via Enrichr	51
4.8	Top Enriched Molecular Function (GO-MF) 2025 for IDO1 via Enrichr	51
4.9	Top Functional Partner Proteins of IDO1	52
4.10	IDO1-interacting transcription factors (immune-related TFs highlighted in blue)	55
4.11	miRNAs interacting with IDO1 as identified through TarBase (NetworkAnalyst)	56

List Of Figures

Figure No	Description	Page #
2.1	IDO protein structure	5
2.2	Structural Representation of IDO1	6
2.3	Tryptophan-Kynurenine (Trp-Kyn) Pathway and Its Metabolic Derivatives	7
2.4	Environmental factor affecting the IDO1 function	9
4.1	mRNA expression of IDO, retrieved from GEPIA	25
4.2	mRNA expression analysis of IDO across various TCGA cancer types	26
4.3	Expression pattern analysis of IDO in different cancers using GENT2 server	27
4.4	Expression of IDO in subtype of liver cancer	28
4.5	Comparison of IDO expression in LIHC and normal tissues	29
4.6	Based on TCGA dataset, the expression of IDO was retrieved from UALCAN	30
4.7	Expression of IDO based on clinicopathological parameters in LIHC	32
4.8	mRNA expression of IDO in LIHC based on patient's race, as retrieved through UALCAN.	32
4.9	mRNA expression of IDO in LIHC based on patient's age, as retrieved through UALCAN.	33
4.10	mRNA expression of IDO in LIHC based on nodal metastasis, as retrieved through UALCAN	33
4.11	mRNA expression of IDO in LIHC based on tumor grade, as retrieved through UALCAN	34
4.12	Overall Survival data analysis, retrieved from GEPIA2	35
4.13	Disease Free Survival Overall data analysis, retrieved from GEPIA2	36

4.14	Overall survival data retrieved from (Tumor Liver Hepatocellular Carcinoma - TCGA - 371 - rsem – tcgars) dataset using R2 platform.	37
4.15	Overall survival data retrieved from (Mixed Liver Hepatocellular Carcinoma (2022-v32) - tcga - 424 - tpm - gencode36) dataset using R2 platform.	38
4.16	Overall survival data analysis from OncoLnc server	39
4.17	Heatmap representing the positively correlated genes with IDO1 in LIHC	40
4.18	Correlation analysis between IDO1 and HLA-DOB using UCSC Xena web tool	42
4.19	Coexpression analysis of IDO1 and HLA-DOB transcript level in LIHC, retrieved from GEPIA2.	43
4.20	Enrichment analysis of IDO, retrieved through Enrichr	44
4.21	IDO interacting network of proteins, retrieved from STRING database.	48
4.22	IDO interaction network, retrieved from GeneMANIA	49
4.23	The docked pose of IDO1protein with Quercetin ligand	51
4.24	The full image of IDO1- Quercetin interaction in a 3D representation.	52
4.25	TF-network of IDO, generated from ChEA database using NetworkAnalyst platform	53
4.26	miRNA network of IDO, generated from TarBase database using NetworkAnalyst platform	54
4.27	Evaluation of diagnostic value of IDO gene	55
4.28	Evaluation of prognostic value of IDO gene	56

List Of Abbreviation

IDO1	Indolamine 2,3-dioxyeganse 1
GBM	Glioblastoma multiforme
HNSC	Head and Neck squamous cell carcinoma
KICH	Kidney Choromophobe
KIRC	Kidney renal clear cell carcinoma
LIHC	Liver hepatocellular carcinoma
LUAD	Lung adenocarcinoma
LUSC	Lung squamous cell carcinoma

ABSTRACT

Cancer is the predominant cause of death around the world. Thus, identifying suitable biomarker is important to overcome this burden. This study was aimed to study whether Indoleamine 2, 3-dioxygenase (IDO) could serve as a diagnostic and prognostic cancer biomarker and to explore if the IDO's protein-protein interaction plays any role in its biomarker activity using various bioinformatics tools. IDO1 expression in cancer, the clinicopathological analysis of IDO1, correlation analysis between IDO1 expression and survival probability in cancer patients, co-expression analysis of IDO gene, enrichment and network analyses, molecular modeling analysis, and statistical analysis were performed using GEPIA, UALCAN, GENT2, GEPIA2, R2 platform, OncoLnc server, UCSC Xena, R-Studio, Enrichr, STRING, GeneMANIA, NetworkAnalyst platform, ORCA, Pyrx, and DATAtab online web tool. We found that IDO1 is significantly overexpressed in LIHC across different datasets (GEPIA2, UALCAN, and GENT2), showing correlations with tumor stage, grade, nodal status, and patient age. Its coexpression with HLA-DOB, along with enrichment of tryptophan metabolism and immune-modulatory pathways, supports its role in tumor immune escape. Diagnostic evaluation revealed a high biomarker potential (AUC = 0.91), although its prognostic associations were limited. Furthermore, molecular docking and DFT studies confirmed IDO1's catalytic stability and immune-metabolic relevance. Overall, IDO1 emerges as a robust diagnostic biomarker and therapeutic target in LIHC, highlighting its potential for early detection and immunotherapy strategies. However, further confirmatory studies are required to establish IDO1 as a suitable biomarker.

KEY WORDS:

Biomarker, IDO, Liver cancer, Cancer, Diagnostic

CHAPTER 1
INTRODUCTION

Cancer is the predominant factor leading to mortality worldwide. It is a complex disease characterized by proliferation of cell and metastasis. Cancer is a complex disease which have many types, it continues to challenge the scientific community due to its varied response to the treatments and genetic heterogeneity. Despite progress in therapy and early detection, cancer's heterogeneity presents substantial obstacles. Recently, there have been notable progressions in the management of cancer, leading to the development of individualized and focused treatments. These medicines have effectively postponed the progression of the disease and prolonged the lifespan of patients [1].

There is a need for innovative therapeutic alternatives for widespread or severe disease, specifically for cancer patients, which currently lacks focused treatment choices [2-3]. Checkpoint inhibitors in immunotherapy have demonstrated remarkable clinical efficacy in several types of tumors, such as melanoma and non-small cell lung cancer, and are swiftly revolutionizing the field of medical oncology [4]. Molecular mechanisms play main role in the progression of cancer; role of immune checkpoints have gathered significant attention in this decade. Indoleamine 2, 3 dioxygenase (IDO) enzyme has emerged as crucial player among these checkpoints by exerting significant influence on microenvironment modulation and tumor immune evasion [1].

In 1963, Osamu Hayaishi et al., discovered IDO1 by studying oxygenases in rabbit intestine. In 1998, Mellor and Munn demonstrated that cells producing IDO protect the mammalian fetus from maternal T-cell attack, highlighting IDO's immune tolerance function. This data provided great interest in IDO study. IDO is responsible for the breakdown and processing of tryptophan amino acid and also Tryptophan-IDO-Kynurenine pathway, playing a key role in immune regulation. Tryptophan is an essential amino acid responsible for cell growth and metabolism. Lack of tryptophan results in improper function of immune system. Elevated IDO1 protein expression suppresses the growth and induces apoptosis of T effector cells. The reduction in the number of T effector cells lose their ability to act against cancer cells and enhance their growth. The reduction in T effector cells diminishes their ability to act against cancer cells, thereby

promoting tumor growth. IDO1 has emerged as a key immunotherapy target and is implicated in lung cancer, melanoma, ovarian cancer, leukemia, and other solid tumors. The major enzymes involved in the tryptophan–IDO–kynurenine pathway are IDO1, IDO2, and tryptophan 2,3-dioxygenase (TDO). The activity of these enzymes leads to excessive production of kynurenine, resulting in tryptophan depletion, which in turn weakens the immune system. The tryptophan–IDO–kynurenine pathway produces metabolites such as kynurenine, kynurenic acid, and quinolinic acid. Due to the increased expression of these enzymes, tryptophan molecules are rapidly metabolized, leading to tryptophan deficiency and subsequent inhibition of T cells. This phenomenon suppresses the central nervous, immune, and reproductive systems. Ultimately, this pathway plays a major role in immune suppression within the tumor microenvironment [4-8].

AIMS AND OBJECTIVES

- To explore the importance of IDO as a biomarker in cancer prediction.
- To analyze genomically if IDO can potentially serve as a clinicopathological biomarker for any or several cancer prognosis.
- To determine the Protein-protein interactions of IDO to explore the potential for unravelling biological mechanisms and developing therapeutic interventions.

CHAPTER 2
LITERATURE REVIEW

2.1. Background

Cancer is the predominant factor leading to mortality worldwide. It is a complex disease characterized by uncontrolled cell proliferation and metastasis. Early detection in combating the disease remains a significant hurdle. The current goal in this field is to investigate biomarkers for early detection of cancer. However, the biomarkers typically used show low sensitivity and specificity in the early stages of disease [1].

It is now well established that the expression of immunosuppressive molecules influences prognosis, metastatic potential, and the response to cytostatic treatment. Among these molecules, indoleamine 2,3-dioxygenase (IDO) is overexpressed in a wide range of cancers, including colorectal, gynecological, lymphoma, and melanoma. Moreover, its expression by either immune system cells or tumor cells can modulate therapeutic efficacy and promote immune escape, potentially leading to systemic immunotolerance [2–8].

IDO is an inducible heme-containing enzyme that catalyzes the oxidative cleavage of the essential amino acid tryptophan into N-formylkynurenine, which is then rapidly converted to L-kynurenine through the kynurenine pathway. This pathway plays a pivotal role in immune regulation, as depletion of tryptophan and accumulation of kynurenine metabolites suppress effector T-cell activity while promoting regulatory T-cell differentiation. Consequently, IDO has been increasingly recognized as a key modulator of tumor-induced immune suppression and as a potential therapeutic target. Given its critical role in tumor immune evasion, IDO has also emerged as a promising candidate biomarker [9].

2.2. Introduction To IDO

Indoleamine 2,3-dioxygenase 1 (IDO1) is an intracellular, heme-containing cytosolic enzyme composed of 403 amino acids that catalyzes the oxidative cleavage of the indole ring of L-tryptophan to form N-formylkynurenine, the first and rate-limiting step of the kynurenine pathway of tryptophan catabolism [10–11]. IDO1 has been reported to play crucial roles in modulating immune responses, maintaining tolerance, and

regulating inflammation in various conditions, including pathogenic infections, neurological disorders, autoimmune diseases, and cancer progression [11–13].

The IDO1 gene is located on chromosome 8p22 and can be transcriptionally upregulated by interferons (IFNs), particularly IFN-γ, through its promoter region, which contains interferon-stimulated response elements (ISREs) and gamma-activated sequences (GAS), allowing fine-tuned regulation depending on the cellular context [12–14].

Historically, IDO1 was first identified as part of the host defense mechanism against pathogens, including viral and parasitic infections [15]. However, accumulating evidence indicates that beyond pathogen control, IDO1 contributes to the establishment of acquired immunological tolerance, where it depletes local tryptophan levels and increases kynurenine production, leading to T-cell anergy, regulatory T-cell (Treg) differentiation, and natural killer (NK) cell suppression. These mechanisms have been strongly implicated in tumor immune escape, where cancer cells exploit IDO1 activity to evade anti-tumor immunity [14–17].

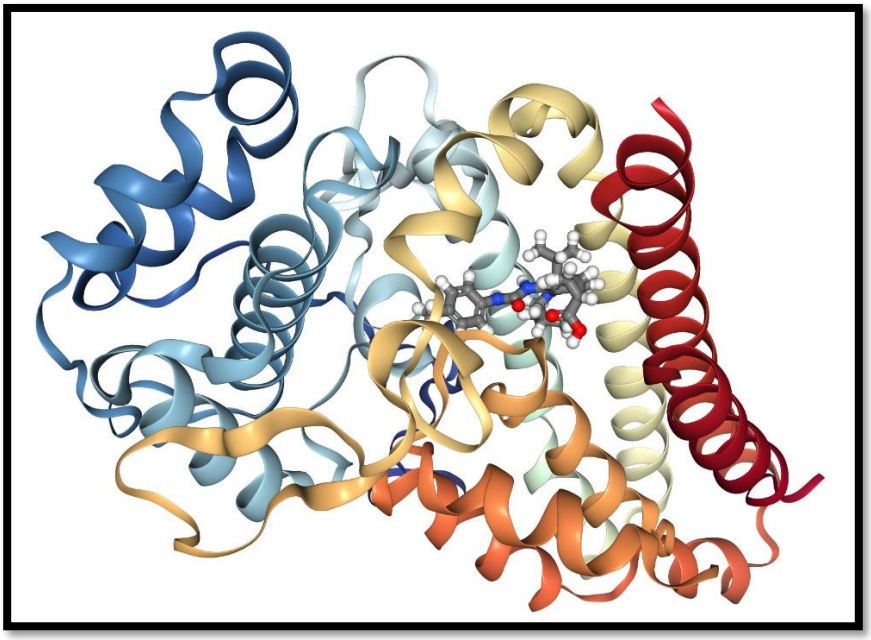


Fig 2.1: 3D structure of IDO protein. The IDO secondary structure can be represented by colors: i.e., red and golden yellow color shows the alpha-helices and blue and light-yellow color shows the beta-sheets. This figure emphasizes the functional domains of IDO and complexity of its structure.

The enzyme was first discovered in the intestinal tract of rabbits. The IDO protein

exists in two isoforms: IDO1 and IDO2. Despite being situated in close proximity, these genes possess unique molecular characteristics that determine their particular activities. In the cytosol of several organs including the lungs, spleen, liver, kidneys, and brain, IDO1 is a crucial component in immune control. In contrast, IDO2 is expressed at much lower levels and with higher selectivity than IDO1, placing IDO1 as the more extensively researched isoform [18,19].

2.3. Structure Of IDO

IDO1 is a 45-kiloda polypeptide enzyme which operates as a monomer and contains a heme tail.

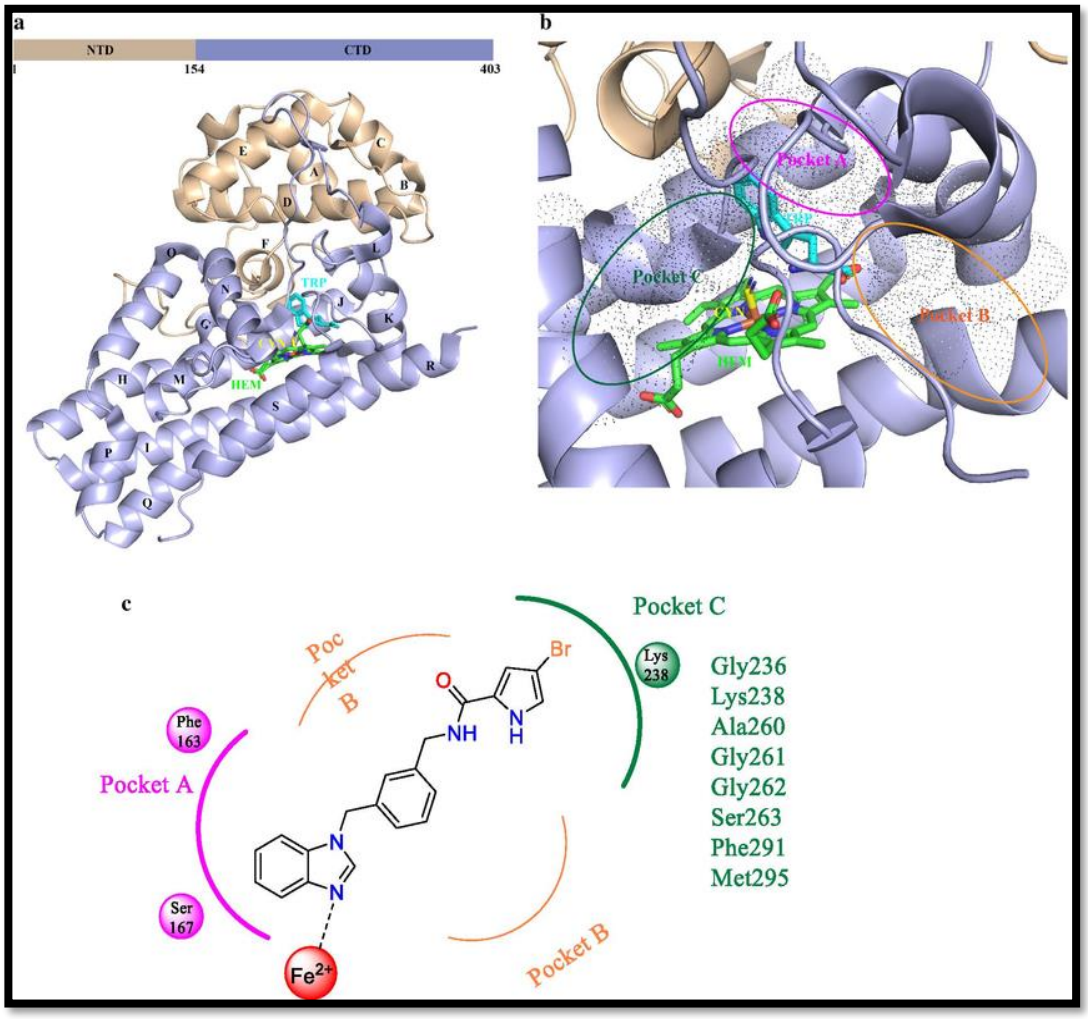


Fig 2.2: Structural Representation of IDO1: (a) IDO's structure is shown, aurantium ribbon represents N-terminal and purple ribbons represent C-terminal domain, respectively. A to S helices are labeled according to their order in primary sequence. Tryptophan is represented in sky blue color while the Heme cite is represented in green color. The active sites of IDO1 gene (three distinct pockets) are represented by

magenta, orange and jasper color for pocket A, B and C respectively (Gao et al.,2009).

A crucial function of IDO1 in the kynurenine pathway is to catalyze the oxidative cleavage of the 2,3-double bond in tryptophan's indole ring, incorporating one molecule of oxygen to generate N-formyl-kynurenine (N-formyl-Kyn). This unstable intermediate quickly and spontaneously undergoes conversion into kynurenine (Kyn), a pivotal metabolite in tryptophan catabolism. Kynurenine can then be further metabolized into several physiologically active downstream products, including kynurenic acid, anthranilic acid, 3-hydroxykynurenine, and quinolinic acid, which play significant roles in immune regulation, neurotransmission, and redox homeostasis [20].

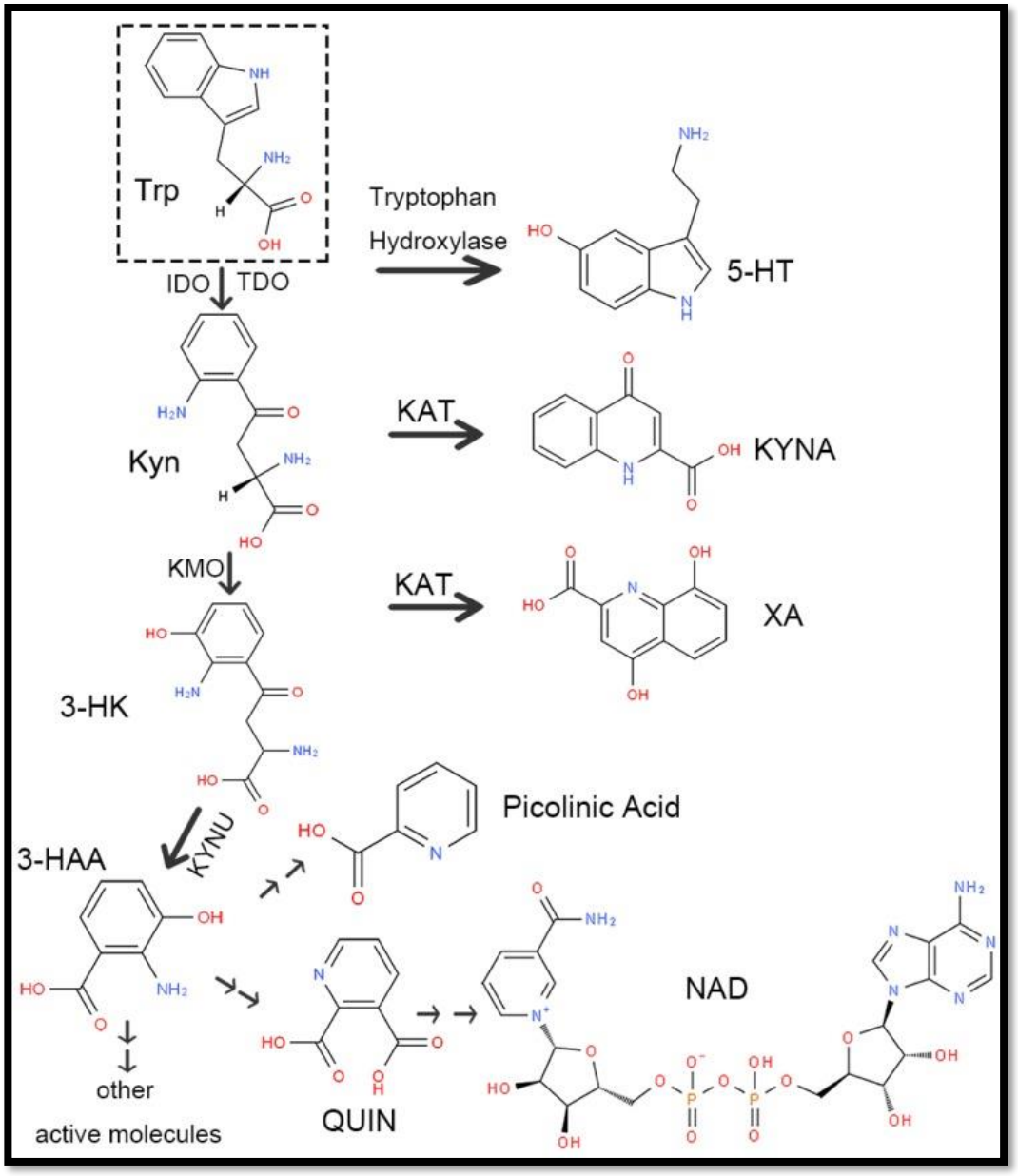


Fig 2.3: Tryptophan-Kynurenine Pathway and Its Metabolic Derivatives: The figure illustrates the metabolic pathway of tryptophan through the kynurenine pathway. IDO and TDO catalyze the conversion of tryptophan to kynurenine. Kynurenine is subsequently metabolized by various enzymes: KAT (kynurenine aminotransferase) leads to the formation of kynurenic acid (KYNA) and xanthurenic acid (XA), while KMO (kynurenine 3-monooxygenase) converts it into 3-hydroxykynurenine (3-HK). Further metabolism of 3-HK by KYNU (kynureninase) produces 3-hydroxyanthranilic acid (3-HAA), which, through further reactions, generates picolinic acid, quinolinic acid (QUIN), and NAD (nicotinamide adenine dinucleotide), crucial molecules in cellular processes. This pathway highlights alternative metabolic fates of tryptophan, including serotonin (5-HT) synthesis via tryptophan hydroxylase, and underscores the role of kynurenine metabolites in cellular function and disease states (Muller A et al.,2016)

The activation of IDO1 occurs when heme is in the Fe^{3+} state. Enzyme's active site consists of two hydrophobic regions: a gateway to the binding site and a spacious inner cavity housing the heme group, which functions as the catalytic site for tryptophan (Trp). The crystal structures of IDO1 have been identified as two distinct: one bonded to cyanide and the other bonded to 4-phenylimidazole (4PI) [21-23].

Further investigation reveals that IDO plays a pivotal function in controlling immunological responses by dendritic cells through many methods. For example, Sun et al. (2012) reported that histone deacetylase (HDAC) inhibitors regulate the acetylation and activation of STAT3 in dendritic cells, which in turn enhances IDO expression. Furthermore, IDO has been shown to physically interact with the suppressor of cytokine signaling 3 (SOCS3) in dendritic cells; this interaction promotes degradation of IDO/SOCS3 complexes via proteasomal pathways, thereby modulating immunosuppressive functions [24,25].

2.4. Regulation And Functional Adaptation Of IDO1

The catalytic activity of IDO1 produces its main product, L-kynurenine (a natural ligand of the aryl hydrocarbon receptor), which promotes the differentiation of T cells into Treg cells, thereby regulating the gene expression of IDO1 [26].

In response to environmental conditions, IDO1 can alter its function through conformational changes. Factors such as the redox state of the cell, temperature variations, changes in cellular localization, and phosphorylation events contribute to post-translational modifications of IDO1. Moreover, IDO1 interacts with signal transducers that reprogram dendritic cell (DC) functions and induce genomic effects. The expression of IDO1 can be either reduced or sustained through phosphorylable ITIMs (Immunoreceptor Tyrosine-based Inhibitory Motifs) [27,28].

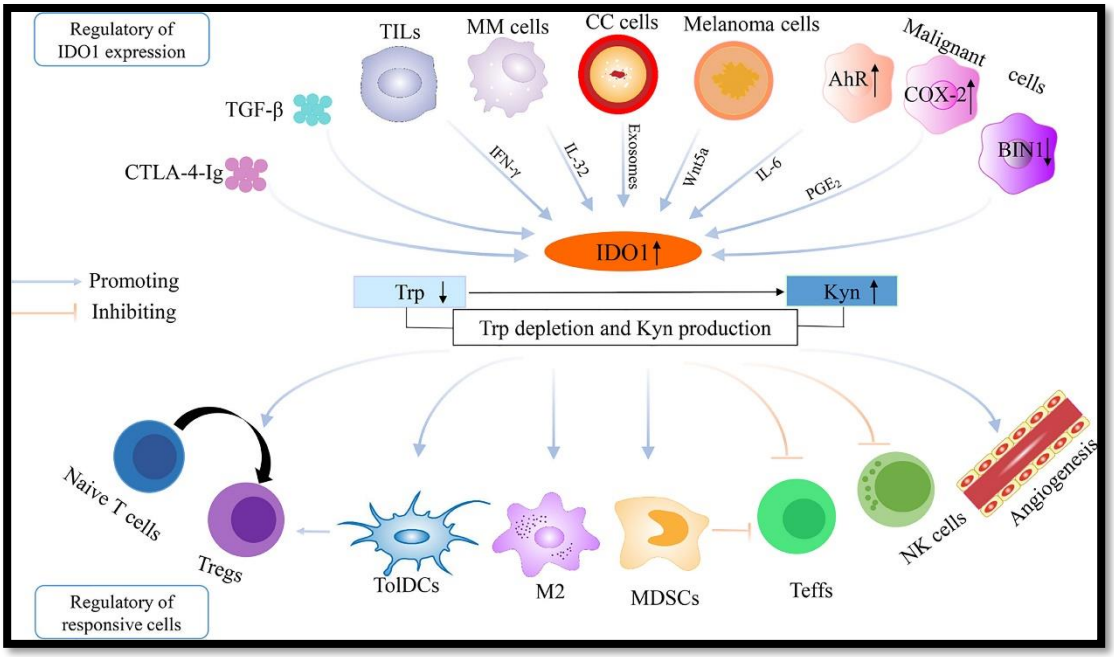


Fig 2.4: Mechanisms of IDO1 regulation and immunosuppressive effects in the tumor microenvironment. The figure illustrates that IDO1 expression is regulated by tumor-infiltrating lymphocytes (TILs), multiple myeloma (MM) cells, colorectal carcinoma (CC) cells, melanoma cells, and malignant cells through cytokines (e.g., IFN-γ, IL-32, IL-6), signaling molecules (TGF-β, CTLA-4-Ig, Wnt5a, PGE_2), and transcriptional regulators (AhR, COX-2, BIN1). Upregulation of IDO1 promotes tryptophan depletion and kynurenine accumulation, which in turn suppress effector T cells (Teffs) and natural killer (NK) cells, while promoting regulatory T cells (Tregs), tolerogenic dendritic cells (TolDCs), myeloid-derived suppressor cells (MDSCs), and M2 macrophages. This immunosuppressive cascade facilitates tumor immune evasion, angiogenesis, and systemic immune tolerance (Platten et al.,2012).

2.5. The Role Of IDO1 In Cancer Progression And Immune Evasion

Elevated IDO1 expression is linked to unfavorable prognosis in several types of malignancies because of its function in promoting immunological tolerance. The IDO1 protein promotes the advancement of cancer by several mechanisms:

Role of IDO1 in Tumor Immune Escape:

IDO1 facilitates the development of tolerogenic antigen-presenting cells (APCs), thereby enhancing tolerance toward tumor-associated antigens (TAAs) and supporting tumor growth. Expression of IDO1 in APCs within tumor-draining lymph nodes allows malignant cells presenting TAAs to evade immune surveillance [30].

Regulation via the Kynurenine Pathway:

Through the kynurenine pathway, IDO1 modulates immune responses by

depleting local tryptophan and generating kynurenine (Kyn) metabolites. This mechanism inhibits the cytotoxic activity of natural killer (NK) cells and CD8+ T cells while simultaneously promoting the expansion of regulatory T cells (Tregs) and myeloid-derived suppressor cells (MDSCs). Moreover, kynurenine acts via the aryl hydrocarbon receptor (AhR) and general control non-depressible 2 (GCN2) pathway, leading to inhibition of the mammalian target of rapamycin (mTOR) signaling cascade. Tryptophan depletion further hinders the proliferation of NK and effector T cells, whereas toxic Kyn metabolites trigger T-cell apoptosis and suppress differentiation of T-helper 17 (Th17) cells [30].

Induction of MDSCs and Angiogenesis:

IDO1 also accelerates the expansion and recruitment of MDSCs, which suppress NK cells and T-cell functions while facilitating tumor cell migration. Tumor-associated MDSCs infiltrate the tumor microenvironment and establish a strongly immunosuppressive milieu. Furthermore, IDO1 contributes to angiogenesis by reducing IFN-γ levels and enhancing IL-6 secretion, thereby promoting cancer progression [30].

2.6. Cancer Biomarker

Cancer biomarkers (CBs) are biomolecules synthesized either by cancer cells themselves or by normal physiological cells in response to the presence of a tumor. Each cell type possesses a unique molecular signature, defined by the specific expression levels or functions of distinct genes, proteins, or other molecular features. This uniqueness enables biomarkers to play a central role in the molecular detection of cancer. Cancer biomarkers can be applied in screening, early detection, diagnosis, prognosis, and prediction of clinical outcomes. Moreover, they help in identifying patient subgroups that are more likely to respond to specific therapeutic interventions [31–34].

The spectrum of biomarkers includes genes, gene products, cell populations, enzymes, hormones, and small molecules, which can be detected in blood, urine, tissues, or other human fluids [35]. A cancer biomarker is thus a measurable attribute that signals the likelihood, presence, or treatment response of a tumor. These features may be molecular, cellular, physiological, or imaging-based.

Molecular and cellular cancer biomarkers, present in body fluids or tissues, can be secreted by both healthy and malignant cells in response to cancer development.

Oncological biomarker testing involves the analysis of tumor samples or liquid biopsies to detect alterations in proteins, RNA, DNA, metabolites, or other biomolecules. The information obtained is essential for applications in precision oncology, including treatment selection, disease monitoring, prognosis, early diagnosis, and prediction of drug responses [36].

A broad spectrum of therapeutic applications exists for cancer biomarkers, with the overarching goal of advancing precision medicine to improve cancer prevention, screening, and treatment strategies. These include risk assessment, screening and early detection, accurate diagnosis, prognosis prediction, forecasting therapeutic responses, and monitoring disease progression and treatment efficacy [37–39].

2.7. Screening And Early Cancer Detection Biomarkers

The purpose of these indicators is to detect cancer in apparently healthy persons who have not exhibited any symptoms. Their indication of the possible existence of cancer necessitates subsequent confirmation by other medical techniques. The main justification for adopting these biomarkers is that the timely identification of cancer, especially during periods without symptoms, might enhance patient survival rates and decrease the probability of complications or adverse health outcomes. Nevertheless, there are cases in which the utilization of these biomarkers can result in overdiagnosis, characterized by the identification of a malignancy that would not have induced any symptoms or damage [40-45].

2.8. Accurate Cancer Diagnosis Biomarkers

In order to verify the existence of cancer or to pinpoint particular subtypes of cancer, diagnostic biomarkers are utilized. Their main advantage is that a precise diagnosis can direct suitable therapy, therefore enhancing the likelihood of survival. Although diagnostic biomarkers are essential in identifying cancer or categorizing individuals into subtypes, they are insufficient for a definitive diagnosis and should be employed alongside other diagnostic techniques, such as imaging or biopsies [46].

2.9. Prognostic Biomarker

Following the diagnosis of a tumour, a prognostic biomarker offers valuable information about the probable trajectory of the disease, encompassing its likelihood of recurrence, advancement, and the patient's overall survival, regardless of the treatment

administered. Biomarkers can occasionally serve as indicators of tumour load, thereby assisting in the determination of the cancer stage, such as its classification based on tumor-node-metastasis correlation. Prognostic biomarkers commonly identified include protein biomarkers and gene expression signature tests [45-49]. Furthermore, genetic modifications can support the precise categorization of patients with acute leukaemia according to their risk and related consequences [44]. These biomarkers can provide clinicians with valuable information to determine the need for more intensive or prolonged therapies [50].

2.10. IDO1 As A Biomarker In Colorectal Cancer: Diagnostic and Prognostic Insights:

Annually, nearly one million new cases of colorectal cancer are reported worldwide, resulting in half a million fatalities. Despite being in the early stages, this form of cancer often manifests with no symptoms. To reduce its mortality rate, developing new diagnostic tools for its early detection become a great challenge. In recent years, researchers suggested a wide variety of markers for colorectal cancer diagnosis. Studies has also demonstrated the potential utility of IDO activity or its metabolites as biomarkers for cancer. Cavia-Saiz et al. (2014) conducted an analysis for the evaluation of plasma L-kynurenine level's potential as a prognostic biomarker for colorectal cancer patients. The IDO activity was evaluated by comparing the plasma concentration of L-kynurenine in colon cancer patients with that of healthy controls, yielding significant results [40].

Microsatellite instability-high (MSI-H) colorectal cancer exhibits a robust immune microenvironment due to the abundance of tumor-specific neoantigens. Lee et al. (2018) investigated the prognostic impact of these immune features in MSI-H colon cancer patients who underwent curative surgery. Their study evaluated tumor-infiltrating immune cells (TIICs) and the expression of immune checkpoint proteins that may hold therapeutic potential in immunotherapy. Immunohistochemistry confirmed the status of inhibitory receptors, and importantly, higher expression of IDO1, LAG3, and CD274 (PD-L1) in TIICs correlated with improved prognosis among MSI-H colon cancer patients. These findings suggest that targeting these immune checkpoint molecules could provide new therapeutic opportunities.

Another important factor in colorectal cancer progression is Fusobacterium nucleatum (Fn), an anaerobic bacterium known to promote colorectal cancer cell migration. Xue et al. [43] examined its interaction with THP-1-derived macrophages (dTHP1) and investigated its relationship with IDO1 expression. They observed that IDO1 levels were elevated in Fn-infected dTHP1 macrophages, leading to an IDO1-induced metabolic environment characterized by reduced tryptophan (Trp) concentrations and increased kynurenine (Kyn) levels. This metabolic shift inhibited the intracellular proliferation of Fn within dTHP1 cells. Furthermore, IDO1 expression reduced peripheral blood lymphocyte activity, which normally protects macrophages against Fn infection.

These findings collectively suggest that while IDO1 activity may suppress bacterial proliferation, it simultaneously dampens host immune cell function. Thus, inhibition of IDO1 in tumor immunotherapy could potentially worsen Fn-associated infections in colorectal cancer patients.

2.11. IDO1 Expression And Its Regulation In Breast Cancer:

Wei et al. [44] conducted an in-depth investigation of IDO1 expression in breast cancer cell lines and quantified levels of tryptophan (Trp) and kynurenine (Kyn) found in MCF-7 cell supernatants; their study suggested IDO1 promoted angiogenesis. Furthermore, Patterson [45] noted how expression of IDO1 can be negatively regulated by estrogen receptor alpha (ER), suggesting its positive role as an angiogenesis promoter. An examination of 14 breast cancer datasets showed that the expression of IDO1 was reduced in tumours that expressed the oestrogen receptor (ER) compared to tumours that did not express the ER. A hypothesis was put up suggesting that the ER could inhibits IDO1 production by aiding in the methylation of IDO1 promoter.

2.12. IDO Expression And Its Association With Melanoma Progression

According to Rubel et al. [46], IDO1 expression in primary human melanoma cells was found to be associated with Breslow thickness, the presence of tumor-infiltrating lymphocytes, and the degree of peritumoral inflammatory infiltration.

2.13. IDO And Immune Regulation In Gastric Cancer

Nishit and colleagues [20] established a correlation between IDO1 and the expression of TGF-β. Studies in stage 3 gastric cancer patient who had undergone curative resection revealed a correlation between TGF-β expression and Foxp3 expression.

To explore the clinical and prognostic relevance in gastric carcinoma, Liu et al. performed experiment of flow cytometry and immunohistochemistry to investigate the expressions of CD8+ T and CD4+ cells, and also the dendritic cells. Additionally, the expressions of IDO and FoxP3 were investigated separately. An intricate interplay exists among the humoral immune factors and immunocompetent cells were reported. These elements influence the progression and the survival of gastric cancer [13].

2.14. IDO1 Expression And Prognosis In Pancreatic Cancer

Zhang and his coworkers discovered that elevated IDO expression in pancreatic cancer is associated with a negative prognosis, with individuals exhibiting lower IDO1 expression having improved survival outcomes [51].

2.15. IDO1 Expression In Endometrial Carcinoma And Its Association With PD-L1

Evidence of IDO1 expression has also been observed in endometrial cancer. In their study, Mills et al. (2018) evaluated the expression of IDO1 in 60 samples of endometrial cancer and examined its correlation with programmed death-ligand 1 (PD-L1). Their findings demonstrated that IDO1 was prominently expressed in endometrial carcinomas, with widespread staining frequently seen in tumours without mismatch repair.

2.16. IDO1 As A Biomarker In Esophageal Adenocarcinoma

Esophageal adenocarcinoma is the fastest-growing cancer in Western countries. Current therapies often fall short, creating a critical need for new treatments. Loeser et al. (2020) analyzed IDO expression in esophageal adenocarcinoma (EAC) using single-protein and multiplex immunohistochemistry, alongside mRNA in situ technology. Their findings underscore IDO1 as an influential biomarker and propose its potential as a therapeutic target, suggesting its significance within EAC as a subtype with superior survival rates.

2.17. Role Of IDO1 In Thyroid Cancer

Moretti et al. [51] reported that elevated IDO1 expression is associated with BRAF mutations and RET gene rearrangements (RET/PTC), which activate its production and lead to increased expression and phosphorylation of signal transducer and activator of transcription 1 (STAT1). STAT1 activity was identified as a prognostic indicator for thyroid cancer development. Interestingly, even in cases of tumor progression without

RET/PTC rearrangements, STAT1 activity persisted. Ultimately, STAT1-induced overexpression of IDO1 enables tumors to evade immune surveillance and supports their continuous proliferation [53]."

The systematic review and meta-analysis evidences show that IDO may function as a predictive biomarker and potential predictor of clinicopathology for a range of cancers. Thus, to validate the clinical usefulness of IDO1 in solid tumors, more investigation should be needed [12].

CHAPTER 3

METHODOLGY

3.1. Investigation Of mRNA Expression Levels Of IDO1 Across Different Cancers

3.1.1. IDO1 Expression Using GEPIA:

1. Opened “Google”.
2. Searched for “GEPIA”.
3. Clicked the first link http://gepia.cancer-pku.cn/.
4. Entered “IDO1” in gene query box.
5. Clicked on “GoPIA”.
6. Saved the bar plot of expression profile of IDO among different cancers in PNG format.

3.1.2. IDO1 Expression Using UALCAN:

1. Opened “Google”.
2. Searched for “UALCAN”.
3. Clicked the first link https://ualcan.path.uab.edu/.
4. Clicked on “TCGA”.
5. Typed IDO1 in “Enter the gene symbol” search box then selected the cancer type “Liver hepatocellular carcinoma” from TCGA dataset and clicked on the “Explore” button.
6. Then clicked on “Pan-cancer view”.
7. The Pan-cancer view for IDO1 gene represented by boxplot appeared.
8. Downloaded the boxplot in PNG format.

3.1.3. IDO1 Expression Using GENT2:

1. Opened “Google”.
2. Searched for “GENT2”.
3. Clicked the first link http://gent2.appex.kr/.
4. Clicked on “Search-Gene profile”.
5. In “Search gene” menu, selected the types and terms as tissue and gene symbols respectively then entered the “IDO1” in “Keywords” search bar.
6. Clicked on “Search”.

7. Saved the "Boxplot for gene expression profile across cancer experiments [GPL570 platform (HG-U113_Plus_2)]" in PNG format.

3.2. Analysis Of Differential Expression Of IDO1 In Liver Cancer Versus Healthy Tissue

3.2.1. Differential Expression Of IDO1 In Cholangiocarcinoma Using UALCAN:

1. Opened "Google".
2. Searched for "UALCAN".
3. Clicked the first link https://ualcan.path.uab.edu/.
4. Clicked on "TCGA".
5. Typed IDO1 in "Enter the gene symbol" search box and selected the cancer type "Cholangiocarcinoma" from "TCGA dataset" drop-down menu and then clicked on the "Explore" button.
6. Clicked on "Expression".
7. Selected the option "Sample types" from "IDO1 expression based on" drop-down menu.
8. Downloaded the image by selecting the "download PNG image" from "chart context" drop-down menu.

3.2.2. Differential Expression Of IDO1 In LIHC Using GEPIA2:

1. Opened "Google".
2. Searched for "GEPIA2".
3. Clicked the first link http://gepia2.cancer-pku.cn/.
4. "Expression DIY" was selected from the "Expression Analysis" drop-down menu.
5. Clicked on the "Boxplot" option.
6. Typed "IDO1" in the "Gene A" search bar.
7. LIHC was selected from the "Datasets Selection (cancer name)" then clicked on "Add" button.
8. Clicked on "Plot".
9. Downloaded the boxplot showing IDO1 expression in healthy tissues versus LIHC in PDF format.

3.2.3. Differential Expression Of IDO1 In LIHC Using UALCAN:

1. Opened “Google”.
2. Searched for “UALCAN”.
3. Clicked the first link https://ualcan.path.uab.edu/.
4. Clicked on “TCGA”.
5. Typed IDO1 in “Enter the gene symbol” search box and selected the cancer type “Liver hepatocellular carcinoma” from “TCGA dataset” drop-down menu and then clicked on the “Explore” button.
6. Clicked on “Expression”.
7. Selected the option “Sample types” from “IDO1 expression based on” drop-down menu.
8. Downloaded the image by selecting the “download PNG image” from “chart context” drop-down menu.

3.3. Clinicopathological Analysis Of IDO In LIHC

1. Repeated the steps 1 to 6 of section 3.2.3.
2. From “IDO1 expression based on” drop-down menu, different clinicopathological parameters were selected, including “Cancer stage”, “Patient’s race”, “Patient’s age”, “Nodal metastasis status”, and “Tumor grade”.
3. For each parameter, the corresponding expression plots of IDO1 in LIHC were generated and downloaded by selecting the “download PNG image” option from the “chart context” menu.

3.4. Association Between IDO1 Expression And Prognosis In Cancer Patients

3.4.1. Association Between IDO1 Expression And Probability Of LIHC Patients Using GEPIA2:

3.4.1.1. Retrieved Data On Overall Survival:

1. Opened “Google”.
2. Searched for “GEPIA2”.
3. Clicked the first link http://gepia2.cancer-pku.cn/.
4. “Survival Analysis” was selected from the “Expression Analysis” drop-down menu.

5. Typed “IDO1” in the “Gene A” search bar.
6. “Overall survival” was selected from “Methods” option.
7. Selected the “Median” from “Group cutoff” option.
8. LIHC was selected from the “Datasets Selection (cancer name)” then clicked on “Add” button.
9. Clicked on “Plot”.
10. Downloaded the plot in PDF format.

3.4.1.2. Retrieved Data On Disease Free Survival (DFS):

1. Repeated the steps 1-3 of section 3.4.1.1.
2. “Disease free survival” was selected from “Methods” option.
3. Then repeated the steps 5-8 of section 3.4.1.1.

3.4.2. Association Between IDO1 Expression And Probability In LIHC Patients Through R2 Platform:

1. Opened “Google”.
2. Searched for “R2: Genomic Analysis and Visualization Platform”.
3. Clicked the first link https://r2.amc.nl/.
4. Chose option “Survival (Kaplan- Meier\Cox)” from the list of options available on the left side of the main page.
5. In “Survival analysis using a single dataset” menu, selected the dataset as “Tumor Liver Hepatocellular Carcinoma - TCGA - 371 - rsem – tcgars”.
6. Confirmed the dataset by clicking on the “confirm selection” button.
7. Selected the single gene (Kaplan-Meier) option by drop down menu of the “separate by” option.
8. Then clicked on the “next” button.
9. In the Kaplan-Meier scanner interface, the gene name IDO1 was entered in the “Gene/Reporter” field. The cutoff mode was set to median, and overall survival was chosen from the “Type of Survival” option.
10. Clicked on “next” button.
11. Overall survival graph was saved in PNG format.

12. Repeated the steps 1 to 9 again but selected the dataset as “Mixed Liver Hepatocellular Carcinoma (2022-v32) - tcga - 424 - tpm - gencode36”.

3.4.3. Overall Survival Data Retrieved From Oncolnc Server:

1. Opened “Google”.
2. Searched for “OncoLnc server”.
3. Clicked the first link http://www.oncolnc.org/.
4. Typed “IDO1” in search bar and clicked on “Submit” button.
5. Cox regression results for IDO1 gene were appeared, selected the LIHC from cancers and clicked on the “YES PLEASE” option from “plot Kaplan?”.
6. Selected the “50” as lower and upper percentile and clicked on “Submit” button.
7. The Kaplan plot for IDO1 in LIHC was downloaded in PDF format by clicking on “Go to pdf” option.

3.5 . Co-expression analysis of IDO in LIHC cancer

3.5.1. Retrieval Of Positively Correlated Genes Of IDO1 In LIHC By Using UALCAN:

1. Opened “Google”.
2. Searched for “UALCAN”.
3. Clicked the first link https://ualcan.path.uab.edu/.
4. Clicked on “TCGA”.
5. Typed IDO1 in “Enter the gene symbol” search box and selected the cancer type “Liver hepatocellular carcinoma” from “TCGA dataset” drop-down menu and then clicked on the “Explore” button.
6. Clicked on “Correlation”.
7. Clicked on “View heatmap” option.
8. Downloaded the image by selecting the “download PNG image” from “chart context” drop-down menu.

3.5.2. Correlation Analysis Of IDO1 Gene In LIHC By Using UCSC Xena:

1. Opened “Google”.
2. Searched for “UCSC Xena”.
3. Clicked the first link https://genome.ucsc.edu/.

4. Clicked on “Launch Xena”.
5. Selected the “TCGA Liver Cancer (LIHC)” as study type.
6. Clicked on “TO FIRST VARIABLE”.
7. Column B appeared, the data type was set to “Genomic,” with “IDO1” specified as the gene name. The dataset “Gene Expression” was selected, and clicked on “TO SECOND VARIABLE” option.
8. Column C appeared, the data type was set to “Genomic,” with “HLA-DOB” specified as the gene name. The dataset “Gene Expression” was selected, and clicked on “DONE” option.
9. Downloaded the file in .tsv format.
10. Downloaded and installed R-Studio from https://posit.co/download/rstudio/ for further data analysis.
11. Opened R-studio.
12. Installed and loaded the “ggplot2” package.
13. Imported the downloaded dataset into R.
14. Verified the dataset structure using the “View(x)” function.
15. Constructed a scatter plot to visualize the correlation between IDO1 and HLA-DOB gene expression.
16. The plot generated using “ggplot2” package.
17. Downloaded the plot in PNG format.

3.5.3. Correlation Analysis Of IDO1 Gene In LIHC By Using GEPIA2:

1. Opened “Google”.
2. Searched for “GEPIA2”.
3. Clicked the first link http://gepia2.cancer-pku.cn/.
4. “Correlation Analysis” was selected from the “Expression Analysis” drop-down menu.
5. Typed “IDO1” and “HLA-DOB” in the “Gene A” and “Gene B” search bar respectively and correlation co-efficient was selected as Pearson.
6. LIHC tumor was selected from the “TCGA Tumor (cancer name)” then clicked on “Add” button.
7. Clicked on “Plot”.

8. Downloaded the dot plot of coexpression of IDO1 and HLA-DOB in pdf format.

3.6. Enrichment Analysis Of IDO Using Enrichr

1. Opened “Google”.
2. Searched for “Enrichr”.
3. Clicked the first link https://maayanlab.cloud/enrichr/.
4. Entered “IDO1 gene” in query box.
5. Clicked on “submit”.
6. Clicked on “pathways” tab.
7. The “Pathways” tab was opened. The following pathway databases were individually selected: “BioPlanet 2019”, “Reactome 2022”, “WikiPathways 2024 human”, “KEGG 2021 human”, and “ElsevierPathways” For each database, the top-ranked pathways were identified based on adjusted p-values and combined scores automatically provided by “Enrichr”. The results were downloaded and saved in a text file (.txt).
8. The “Ontologies” tab was opened. The following ontology databases were selected: “Gene Ontology (GO) Biological Process 2023” and “Gene Ontology (GO)Molecular Function 2023”. For each ontology category, the top enriched terms were identified based on adjusted p-values and combined scores automatically provided by “Enrichr”. The results were downloaded and saved in a text file (.txt).

3.7. Evaluation Of IDO Interaction Network

3.7.1. Protein-Protein Interaction Using STRING Database:

1. Opened “Google”.
2. Searched for “STRING” database.
3. Clicked the first link https://string-db.org/.
4. Clicked on search.
5. Typed “IDO1” in “Protein name” search bar and selected “homo sapiens” as organism.
6. Clicked on “Search”.
7. Saved the PPI interaction network in PNG format.

3.7.2. IDO Interaction Network Using GeneMANIA:

1. Opened “Google”.
2. Searched for “GeneMANIA”.
3. Clicked the first link https://genemania.org/.
4. Typed “IDO1” in query box.
5. Clicked on “search” button.
6. Saved the IDO1 gene interaction network in PNG format.

3.8. Network Analysis Of IDO Using NetworkAnalyst

3.8.1. Transcription Factor (TF) Analysis:

1. Opened “Google”.
2. Searched for “NetworkAnalyst” web platform.
3. Clicked the first link https://www.networkanalyst.ca/.
4. Clicked on “Gene List Input”.
5. “H. sapiens (human)” was selected from the “Specify organism” drop-down menu.
6. Set the ID type as “Official Gene Symbol”.
7. Typed IDO1 in search bar.
8. Clicked on “Upload”.
9. Clicked on “Proceed”.
10. From the “Gene Regulatory Network (GRN),” “TF-gene interactions” was selected, followed by clicking on “ChEA3” database.
11. Clicked on “Proceed”.
12. Downloaded the TF-network in PNG image format.

3.8.2. miRNA Network Analysis:

1. Repeated the steps 1-7 of section 3.8.1.
2. “Gene-miRNA interactions” was selected from the “Gene Regulatory Network (GRN)” option, followed by clicking on “TarBase” database.
3. Clicked on “Proceed”.
4. Downloaded the miRNA-network in PNG image format.

3.9 Quantum Chemical Analysis Of IDO1 Active Site Using Density Functional Theory "DFT" Study:

1. Downloaded "ORCA" software from its official website: https://orcaforum.kofo.mpg.de.
2. Unzipped the downloaded files into specific directory.
3. Orca software was installed.
4. For preparing the input file, "Avogadro" software was downloaded.
5. Opened the Avogadro software.
6. Imported the prepared file of protein's active site.
7. Added hydrogen atoms.
8. Optimized the geometry of structure.
9. Clicked on the "Extensions" and selected the "Orca" to generate orca input file for DFT.
10. Selected the following parameters in the interface as:

    Run type: DFT
    Functional: B3LYP
    Basis set: DEF-SVP
    Calculation type: Geometry optimization
    SCF convergence: Tight SCF
    Charge: 0
    Multiplicity: 1

11. Orca input file was generated.
12. Saved the file as ".inp format".
13. For running the orca calculation, opened the "Windows PowerShell".
14. Navigated to the working directory containing generated input file using "cd D:\ORCA-run" command.
15. The following command was used to run the job:
    "D:\ORCA\orca.exe (file name).inp > (file name).out".
16. Output files were generated.
17. Results were analyzed.

3.10. Molecular Docking Analysis

3.10.1. Retrieval Of Ligand From PUBCHEM:

1. Opened “Google”.
2. Pubchem was searched.
3. Clicked on the first link.
4. Gene ID 680C91 was searched.
5. The gene file was downloaded in “PDB legacy format”.

3.10.2. Autodocking Using Pyrx:

1. Opened “Google”.
2. Downloaded the PyRx latest version and opened.
3. Clicked on “load molecule”.
4. The protein file appeared.
5. The macromolecules were created by using Autodock.
6. Clicked on “openbabel”, the ligand was uploaded.
7. Ligand energy was minimized.
8. The file was converted into PDBQT format.
9. Clicked on vina wizard, then on start button.
10. The grid was adjusted and docking was performed.
11. The ligand was downloaded in pdb format.

3.10.3. 2D And 3D Visualization On BIOVIA Discovery Studio:

1. The protein structure and ligand were opened.
2. The ligand was pasted on the protein window.
3. In receptor-ligand interaction, the receptor and ligand were defined.
4. The interaction of 2D and 3D models was observed.

3.11. Statistical Analysis Of Gene Expression And Patient Survival In LIHC

3.11.1. IDO Gene Expression Data Retrieval Through GEO Database:

1. Opened “Google”.
2. Searched for GEO database.
3. Clicked the first link
4. Typed the accession number GSE16515 in search bar.

5. Clicked on “GO”.
6. Clicked on “download the file”.
7. The file was downloaded in .txt format.

3.11.1.1. Evaluation Of Diagnostic Value Of IDO Gene Through ROC Curve:

1. Opened “Google”.
2. Searched for “DATA*tab”* online web tool.
3. Clicked the first link https://numiqo.com/.
4. Upload the downloaded file of expression data.
5. Clicked on “ROC curve” option.
6. Set the patient status as “state variable” and expression values as “test variable”.
7. Selected “1” as a state variable value.
8. Saved the ROC curve of survival data.
9. Calculated the confidence interval (CI) of AUC using the DeLong method:

$$CI=AUC\pm Z\times SE$$

Where standard error (SE)

$$=\sqrt{\frac{AUC*(1-A\cup C)+(n\,positive-1)*(Q1-AUC^2)+(n\,negative-1)*(Q2-AUC^2)}{n\,positive\times n\,negative}}$$

$$Q^1=\frac{AUC}{2-AUC}$$

$$Q^2=\frac{2\times AUC^2}{1+AUC}$$

n positive = 423, n negative =5, and Z is approximately equal to 1.96 [55].

3.11.2. Survival Data Retrieval Through OncoLnc:

1. Opened “Google”.
2. Searched for “OncoLnc” platform.
3. Clicked the first link http://www.oncolnc.org/.
4. Typed “IDO1” in search bar and clicked on “Submit” button.
5. Cox regression results for IDO1 gene appeared, selected the LIHC from cancers and clicked on the “YES PLEASE” option from “plot Kaplan?”.

6. Selected the “50” as lower and upper percentile and clicked on “Submit” button.
7. Clicked on the “click here” to downloaded the survival data of LIHC patients in .txt format.

3.11.2.1. Evaluation Of Prognostic Value Of IDO1 Gene Through ROC Curve:

1. Opened “Google”.
2. Searched for DATA*tab* online web tool.
3. Clicked the first link
4. Upload the downloaded file of survival data.
5. Clicked on “ROC curve” option.
6. Set the patient status as “state variable” and expression values as “test variable”.
7. Selected “0” as a state variable value.
8. Saved the ROC curve of survival data.
9. Calculated the confidence interval (CI) of AUC using the DeLong method:

$$CI=AUC\pm Z\times SE$$

Where standard error (SE)

$$=\sqrt{\frac{AUC*(1-A\cup C)+(n\,positive-1)*(Q1-AUC^2)+(n\,negative-1)*(Q2-AUC^2)}{n\,positive\times n\,negative}}$$

$$Q^1=\frac{AUC}{2-AUC}$$

$$Q^2=\frac{2\times AUC^2}{1+AUC}$$

n positive = 234, n negative =126, and Z is approximately equal to 1.96 [55].

CHAPTER 4

RESULTS

4.1. mRNA Expression Levels Of IDO1 Across Different Cancers

The expression patterns of IDO1 in various cancer studies were analyzed using different tools, including GEPIA: Gene Expression Profiling Interactive Analysis, UALCAN: University of Alabama at Birmingham Cancer data analysis Portal, and GENT2: Gene Expression database of Normal and Tumor tissues 2.

4.1.1. Analysis With GEPIA:

The expression data of IDO was retrieved through GEPIA. The plot indicates that the expression of IDO was regulated in various types of cancers namely, Adrenocortical Carcinoma (ACC), Bladder Urothelial Carcinoma (BLCA), Breast Invasive Carcinoma (BRCA), Cervical Squamous Cell Carcinoma and Endocervical Adenocarcinoma (CESC), Cholangiocarcinoma (CHOL), Colon Adenocarcinoma (COAD), Lymphoid Neoplasm Diffuse Large B-cell Lymphoma (DLBC), Esophageal Carcinoma (ESCA), Glioblastoma Multiforme (GBM), Head and Neck Squamous Cell Carcinoma (HNSC), Kidney Chromophobe (KICH), Kidney Renal Clear Cell Carcinoma (KIRC), Kidney Renal Papillary Cell Carcinoma (KIRP), Liver Hepatocellular Carcinoma (LIHC), Lung Adenocarcinoma (LUAD), Lung Squamous Cell Carcinoma (LUSC), Ovarian Serous Cystadenocarcinoma (OV), Pancreatic Adenocarcinoma (PAAD), Pheochromocytoma and Paraganglioma (PCPG), Prostate Adenocarcinoma (PRAD), Rectum Adenocarcinoma (READ), Sarcoma (SARC), Skin Cutaneous Melanoma (SKCM), Stomach Adenocarcinoma (STAD), Testicular Germ Cell Tumor (TGCT), Thyroid Carcinoma (THCA), Thymoma (THYM), Uterine Corpus Endometrial Carcinoma (UCEC), and Uterine Carcinosarcoma (UCS) (fig 4.1).

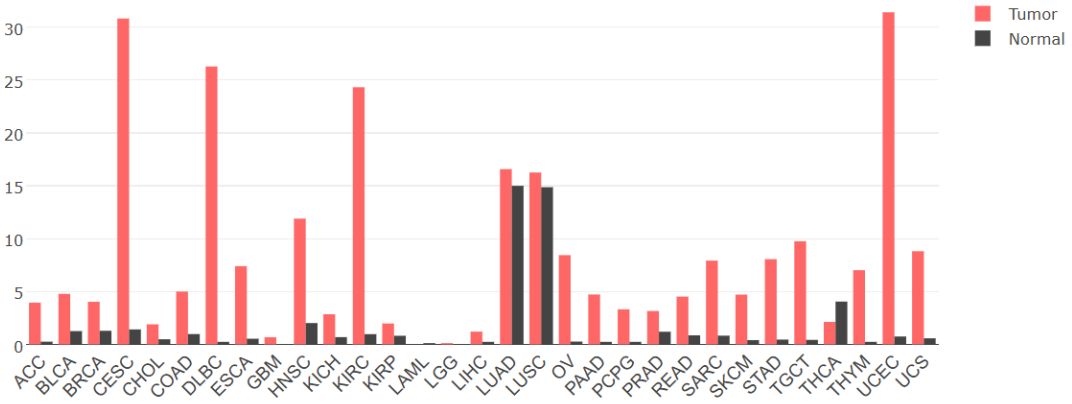


Fig: 4.1: mRNA expression of IDO1 across tumor samples and normal tissues retrieved through GEPIA (Gene Expression Profiling Interactive Analysis). It shows regulation of IDO1 in different cancer types. Y-axis represents the expression of IDO1. The graph shows that IDO1 is highly expressed in CESC (Cervical squamous cell carcinoma) and UCEC (Uterine Corpus Endometrial Carcinoma).

4.1.2. Analysis With UALCAN:

The pan-cancer analysis from UALCAN revealed IDO1 expression across 24 different cancer types. The results indicated upregulation of IDO1 in 18 cancer types, including BLCA, BRCA, CESC, CHOL, COAD, ESCA, GBM, HNSC, KICH, KIRC, KIRP, LIHC, LUAD, PCPG, READ, SARC, STAD, and UCEC. IDO1 was downregulated in 5 cancer types and equally expressed in one cancer type (fig: 4.2).

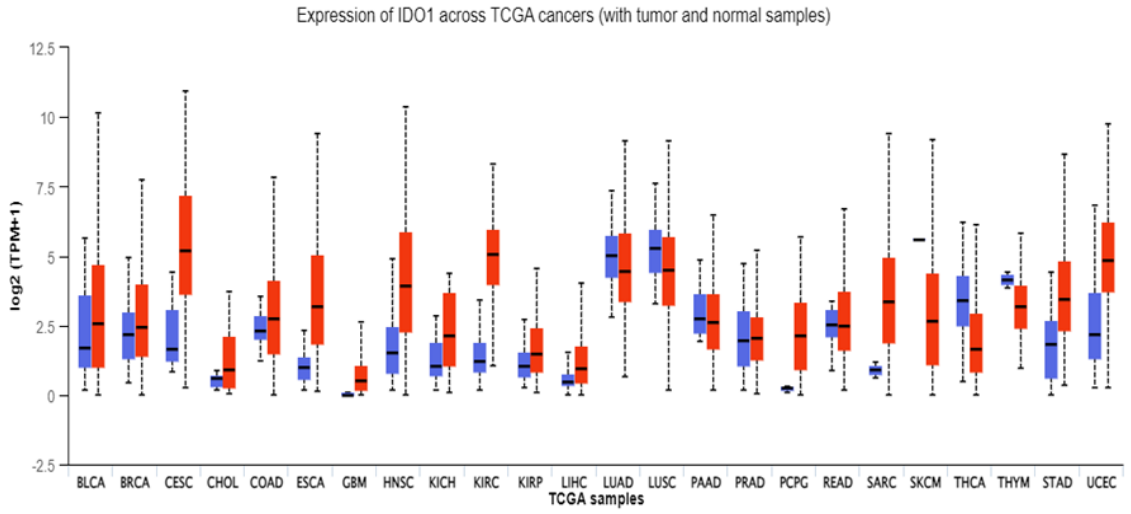


Fig 4.2: mRNA expression analysis of IDO across various TCGA cancer types: The transcription level analysis of IDO1 across various TCGA cancer subtypes paired with normal, *p <0.05, as retrieved from the UALCAN (University of Alabama Cancer Database). tool. The blue boxplots represent normal tissue data, while the red boxplots indicate tumor data. Significant upregulation ($p < 0.05$) was observed in 18 cancer types. IDO1 is highly expressed in CESC (Cervical squamous cell carcinoma). IDO1 was downregulated in 5 cancer types and equally expressed in one cancer type: PRAD (Prostate Adenocarcinoma).

4.1.3. Analysis With GENT2:

The mRNA expression of IDO was re-analyzed using data from independent cohorts of various cancers obtained through the Affymetrix U133Plus2 microarray platform via the GENT2 server, in order to confirm its upregulation across cancer types. The results showed that IDO was upregulated in 26 cancer types, including adipose, adrenal gland, bladder, bone, brain, breast, cervix, colon, esophagus, gallbladder, head and neck, kidney, liver, lymph node, oral, ovary, pharynx, skin, small intestine, spleen, stomach, testis, thyroid, tongue, uterus, vagina, and vulva (fig 4.3).

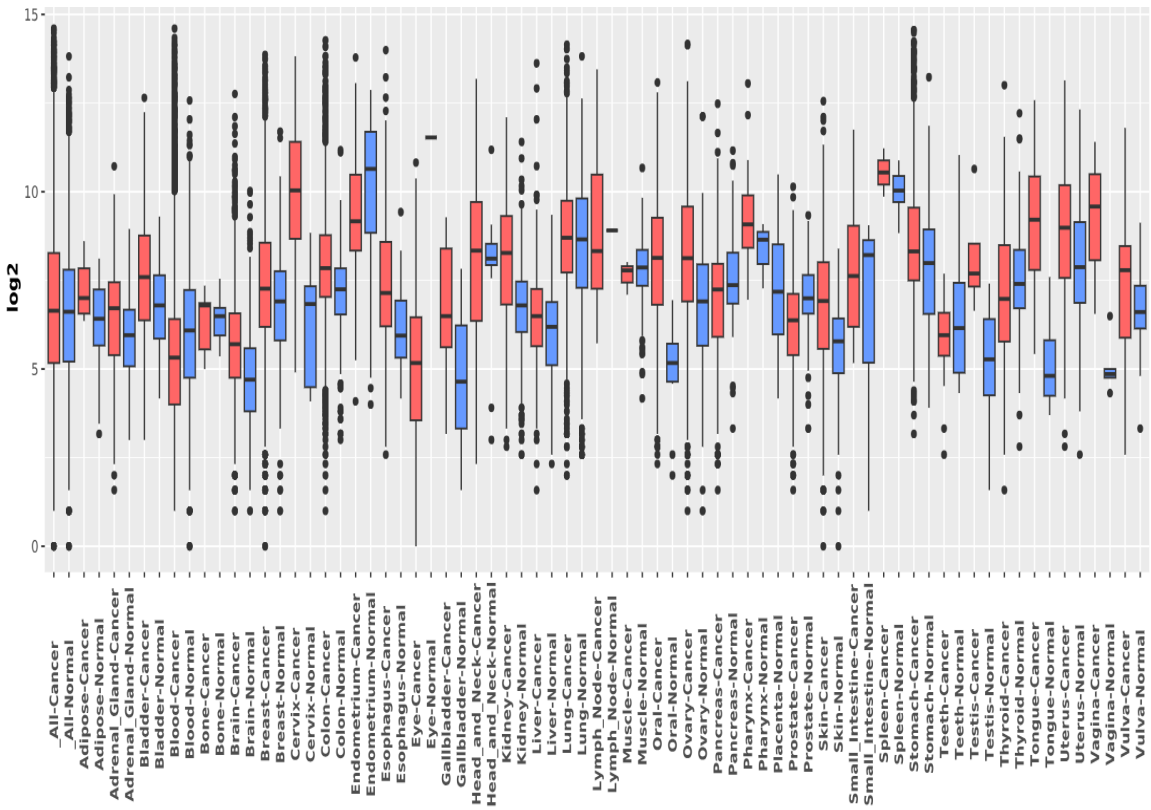


Fig 4.3: Expression pattern analysis of IDO across cancers using the GENT2 (gene expression across normal and cancer tissues 2) server. Validation using Affymetrix U133Plus2 microarray data from independent cohorts confirmed significant upregulation ($p < 0.05$) in 26 cancer types, including adipose, adrenal gland, bladder, bone, brain, breast, cervix, colon, esophagus, gallbladder, head and neck, kidney, liver, lymph-node, oral, ovary, pharynx, skin, small intestine, spleen, and stomach. Blue colour shows the controls, while red indicates the cancerous samples.

4.2. Comparison Of IDO1 Expression In Liver Cancer With Healthy Tissues

4.2.1. Evaluation Of Differential Expression Of IDO1 In Cholangiocarcinoma Using UALCAN:

The IDO expression in cholangiocarcinoma was retrieved through UALCAN and compared with normal controls.The plot indicates the higher expression of IDO in liver cancer subtype (cholangiocarcinoma) compared with normal tissues (fig 4.4).

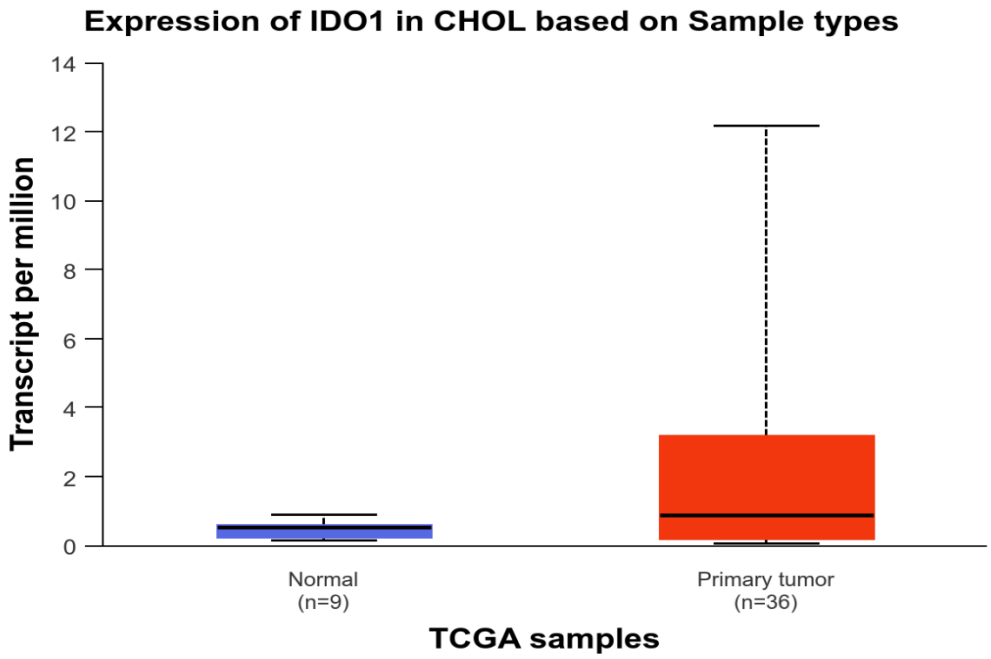


Fig 4.4: The IDO expression in cholangiocarcinoma was compared with the control group was retrieved through UALCAN. The plot indicates the higher expression of IDO in liver cancer subtype (cholangiocarcinoma) compared with normal tissues.

4.2.2. Evaluation Of Differential Expression Of IDO1 In LIHC Using GEPIA2:

Using GEPIA2 and UALCAN tools, the upregulation of IDO1 in LIHC were further assessed. The analysis showed that the expression of IDO1 in LIHC patients was significantly higher as compared to normal tissues (fig 4.5).

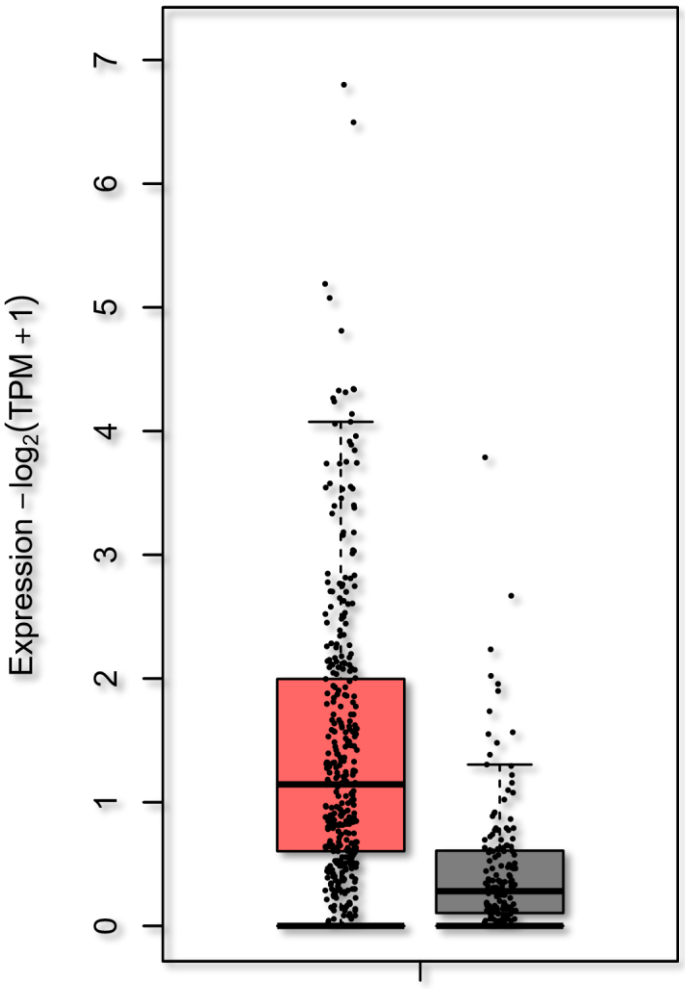


Fig 4.5: Comparison of IDO expression in LIHC and normal tissues was analyzed by GEPIA 2. Boxplot showing IDO1 expression in healthy tissues versus LIHC. Upregulation of IDO1 in Liver Hepatocellular Carcinoma (LIHC) – showed that IDO1 expression was significantly elevated in LIHC patients ($p < 0.05$). In the plots, grey boxplot represents normal tissue expression, while red boxplot represents tumor tissue expression.

4.2.3. Evaluation Of Differential Expression Of IDO1 In LIHC Using UALCAN:

The analysis showed that the expression of IDO1 in LIHC patients was significantly higher as compared to normal tissues (fig 4.6).

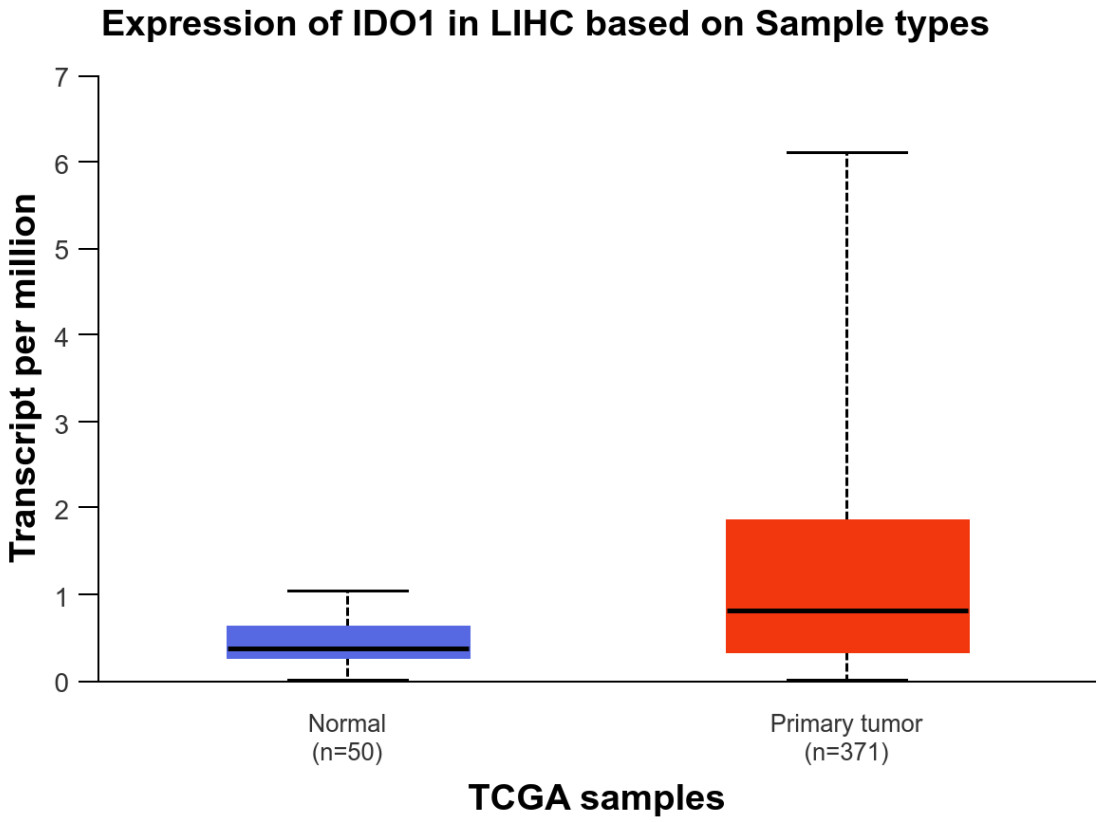


Fig: 4.6: IDO1 expression in Liver hepatocellular carcinoma based on the Cancer Genomic Atlas samples types (TCGA), analyzed using UALCAN. X-axis shows the normal (Blue) and primary tumor (red) samples. Y-axis shows the expression of IDO1. The plot shows upregulation of IDO1 in LIHC.

4.3. Expression Analysis Of IDO1 In Relation To Clinicopathological Parameters In LIHC

Based on the clinicopathological parameters, such as cancer stages, race, age, nodal metastasis status, and tumor grade, the variation in IDO1 expression in LIHC was analyzed using UALCAN tool with default settings. For analysis and interpretation, only statistically significant results were considered ($p < 0.05$). In term of individual cancer stages analysis, IDO1 expression varies when comparing normal tissue with different cancer stages. However, no statistically significant difference in IDO1 expression was observed between normal tissue and Stage 4 cancer, suggesting that IDO1 level may not

increase significantly at the most advanced stage. This finding may show that the changes in expression have reached their peak or limit in the LIHC advanced stage.

In IDO1 expression, significant differences were observed when comparing normal tissues to the early and late stages of cancer, suggesting that IDO1 level increase as LIHC progresses. When comparing Stage 4 to earlier stages, significant differences were also observed, suggesting that IDO1 expression shows potential changes as cancer prognosis to a more advanced stage (Fig: 4.7).

The IDO1 expression is increased in Caucasian and Asian patients in patient's race analysis (Fig: 4.8).

Higher IDO1 expression level was observed in age groups of 41-60, 61-80, and 81-100 years. The analysis indicated that IDO1 expression may be influenced by age, particularly in older patients. The lower IDO1 expression was found in 21-40 years, suggesting that expression may remain stable in younger patients but becomes significantly altered in older ages (Fig: 4.9).

In term of nodal metastasis, the IDO1 expression shows a statistically significant difference in tumors without lymph node involvement (N0), when compared to normal group. On the other hand, N1 do not show significant results. However, the expression of IDO1 is significantly higher in N1 as compared to N0 patients, suggesting its importance as a cancer biomarker for lymphatic involvement in LIHC (Fig: 4.10).

Based on tumor grade, the findings show an increase in IDO1 expression in Grades 1, 2, and 3 tumors compared to normal tissues, indicating that IDO1 may play a role in early to intermediate cancer stages (Fig: 4.11).

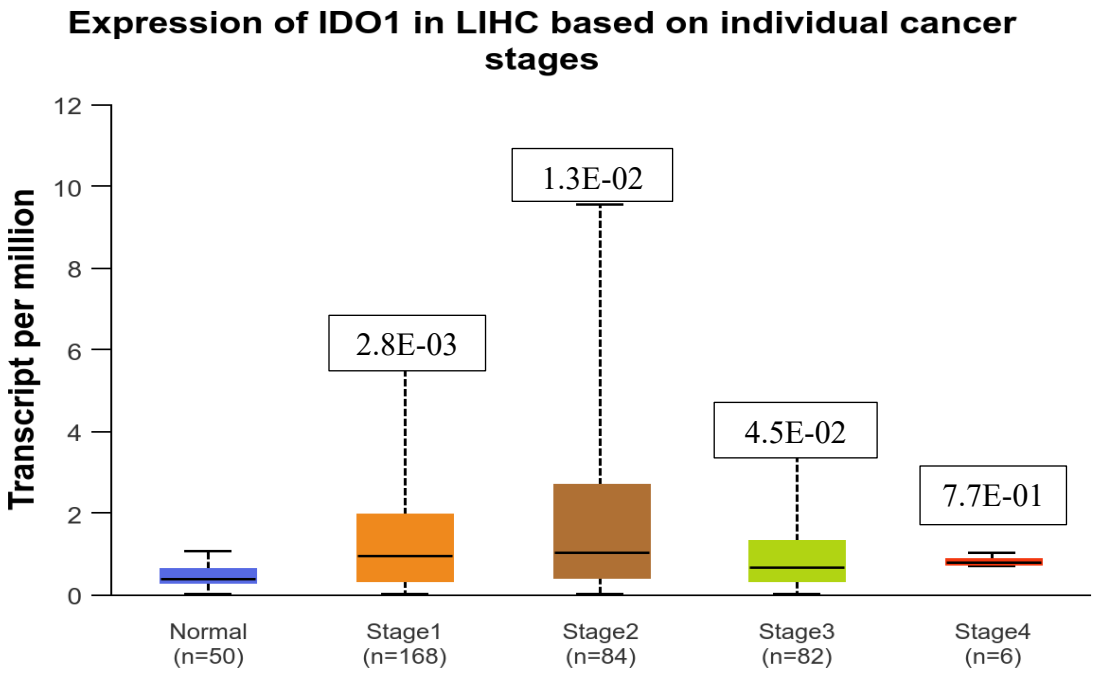


Fig: 4.7: Expression of IDO1 based on individual cancer stages, as retrieved through UALCAN. IDO1 expression was significantly higher in Stages 1–3 compared to normal tissues. No statistically significant difference was observed between normal and Stage 4, suggesting a possible plateau of IDO1 expression in the most advanced stage.

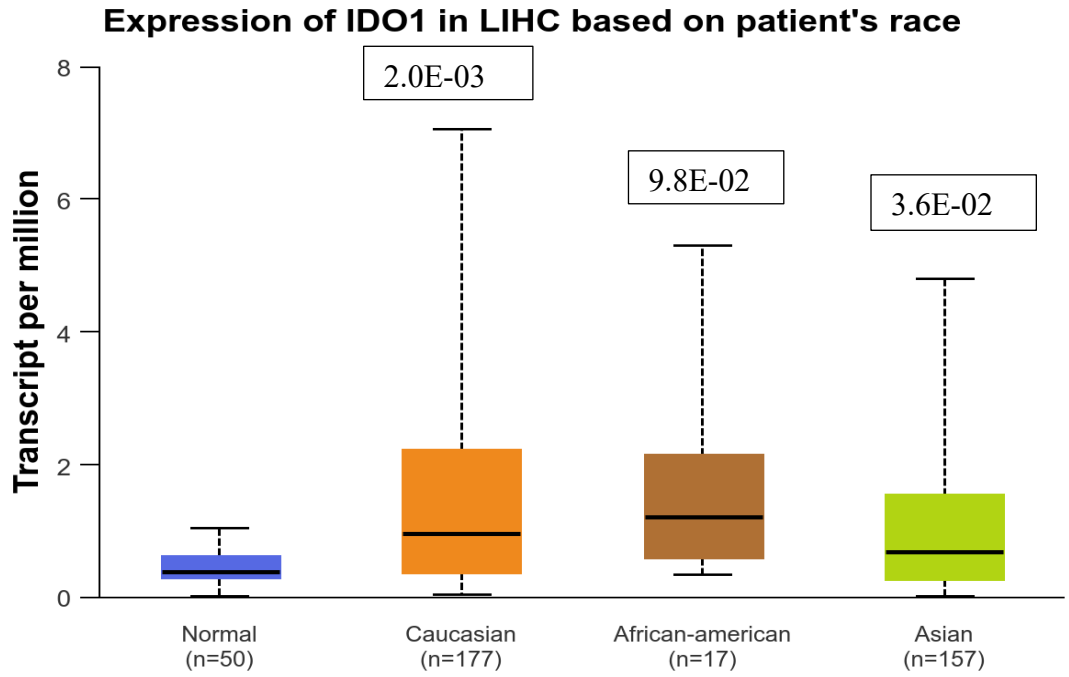


Fig:4.8: IDO1 expression in Liver hepatocellular carcinoma based on the patient's race, analyzed using UALCAN. Elevated IDO1 expression was observed in both Caucasian and Asian patients relative to normal controls.

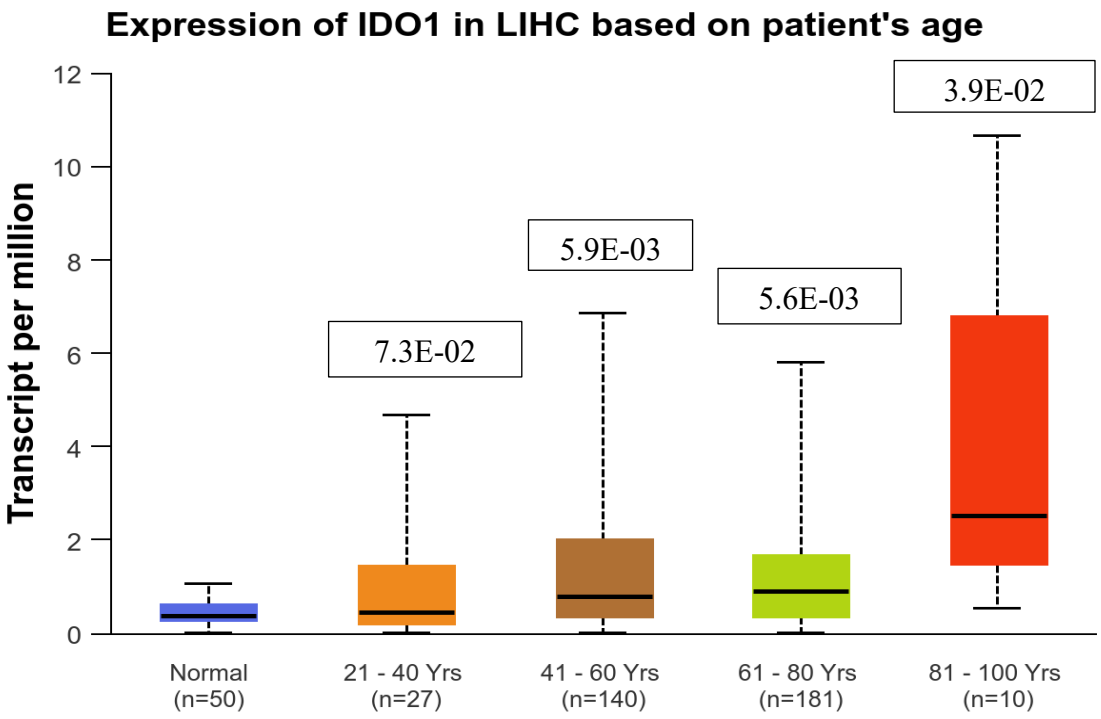


Fig: 4.9: mRNA expression of IDO in LIHC based on patient's age, as retrieved through UALCAN. Higher IDO1 expression levels were detected in the 41–60, 61–80, and 81–100 years age groups, with the lowest expression in the 21–40 years group, indicating an age-related expression trend..

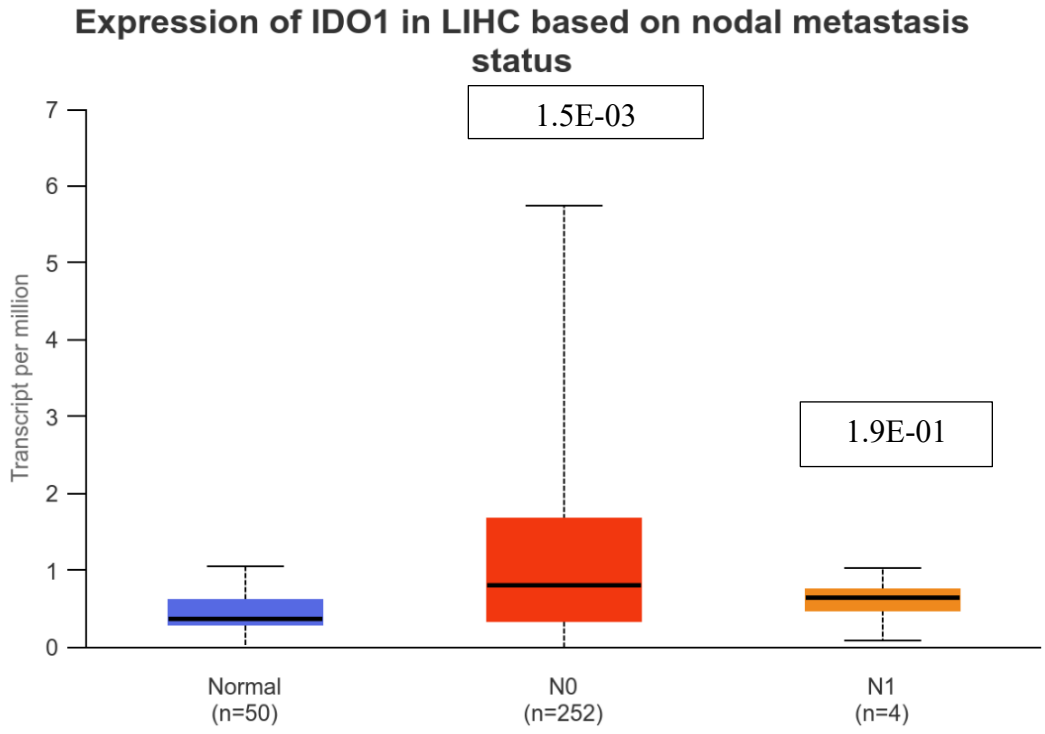


Fig: 4.10: mRNA expression of IDO in LIHC based on nodal metastasis, as retrieved through UALCAN. N0 shows No regional lymph node metastasis and N1 shows Metastases in 1 to 3 axillary lymph nodes.

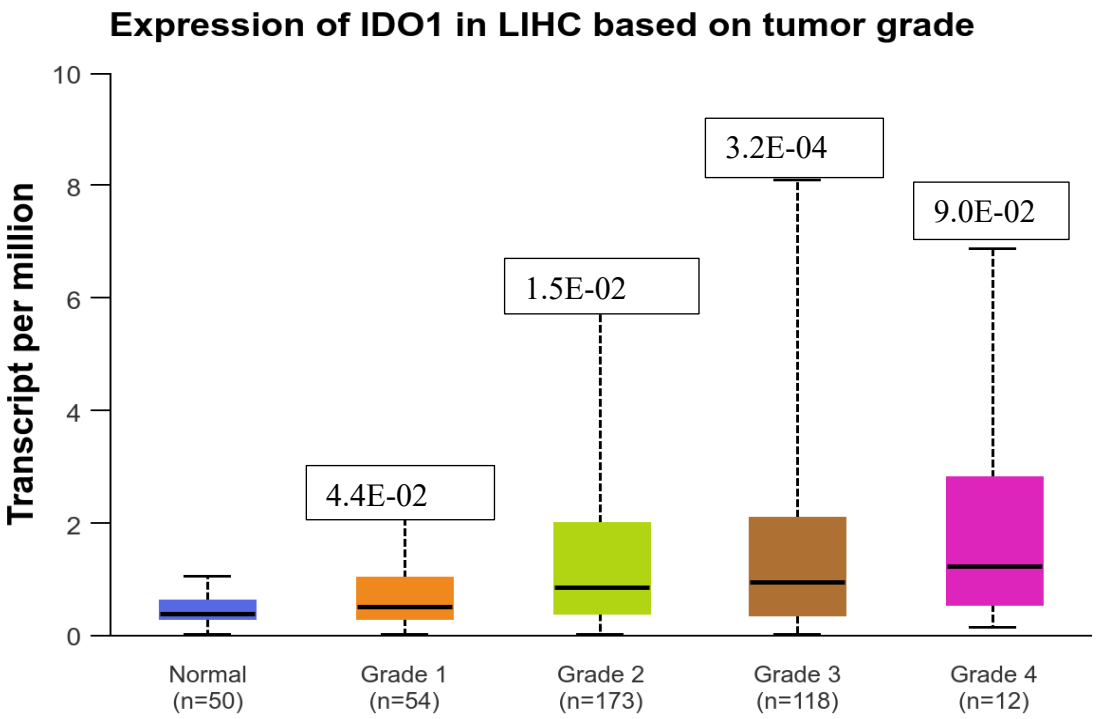


Fig: 4.11: mRNA expression of IDO in LIHC based on tumor grade, as retrieved through UALCAN. Grade 1 represents well differentiated (low grade), Grade 2 represents moderately differentiated (intermediate grade), Grade 3 represents poorly differentiated (high grade), and Grade 4 represents undifferentiated (high grade).

4.4. Correlation Analysis Between IDO1 Expression And Prognosis In Cancer Patients

4.4.1. Association Analysis Between IDO1 Expression And Probability Of LIHC Patients Using GEPIA2:

4.4.1.1. Overall Survival Data Analysis Through GEPIA2:

The Kaplan-Meier survival plot retrieved through GEPIA2. It compares the high and low IDO1 group with overall survival rates. The graph indicates that there is no statistically significant difference between IDO1 expression and survival probability. The hazard ratio indicates that in both cases the risk of death is same (fig: 4.12).

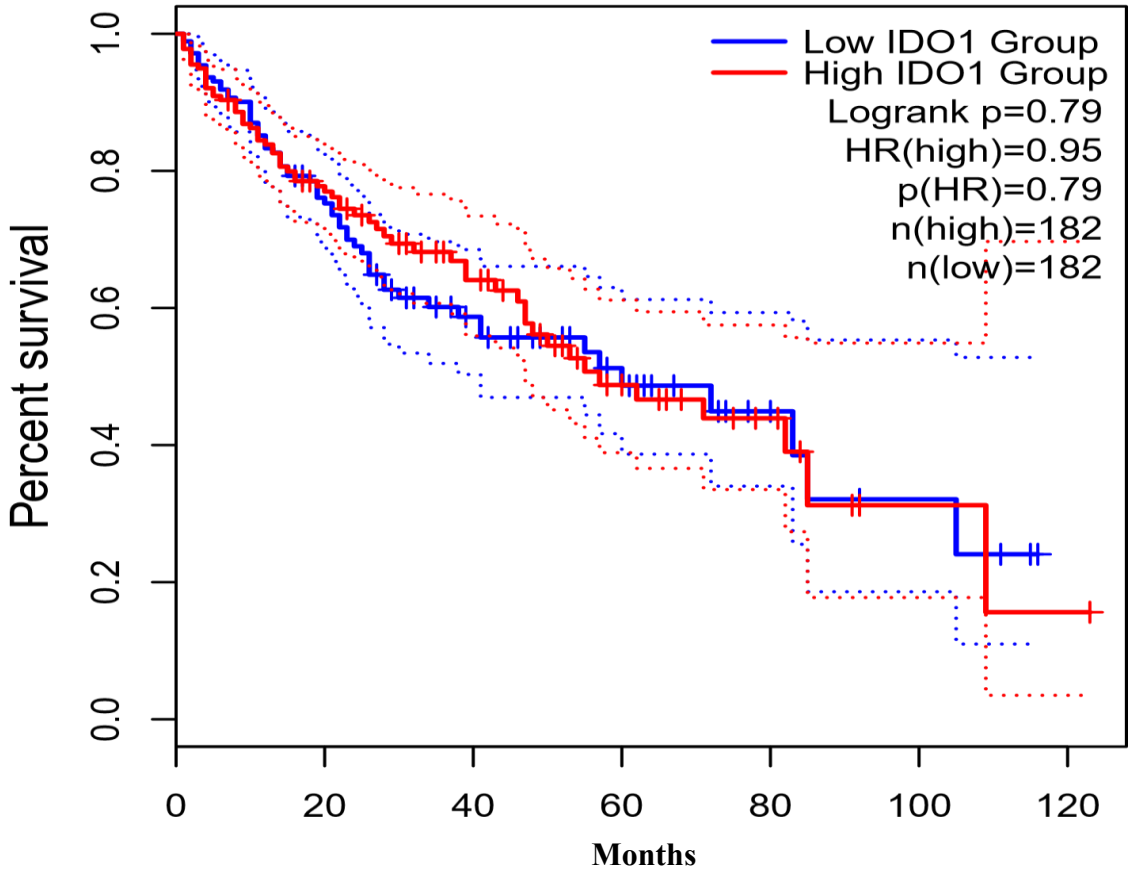


Fig 4.12: Overall Survival data analysis, retrieved from GEPIA2: Blue line represents the group having low IDO1 expression, red line represents the group having high IDO1 expression, and blue and red dotted lines show the 95% confidence intervals for each group. X-axis represents the follow-up duration in months (time), whereas Y-axis represents the survival probability of patients (percent survival), starting at 100% and decreasing over time.

4.4.1.2. Disease-Free Survival Analysis Through GEPIA2:

The Kaplan-Meier disease-free survival plot retrieved through GEPIA2. It compares the high and low IDO1 group with disease-free survival rates. The graph indicates that there is no statistically significant difference between IDO1 expression and disease-free survival. The high hazard ratio indicates that high IDO1 expression is associated to a slightly lower risk of disease reoccurrence (fig: 4.13).

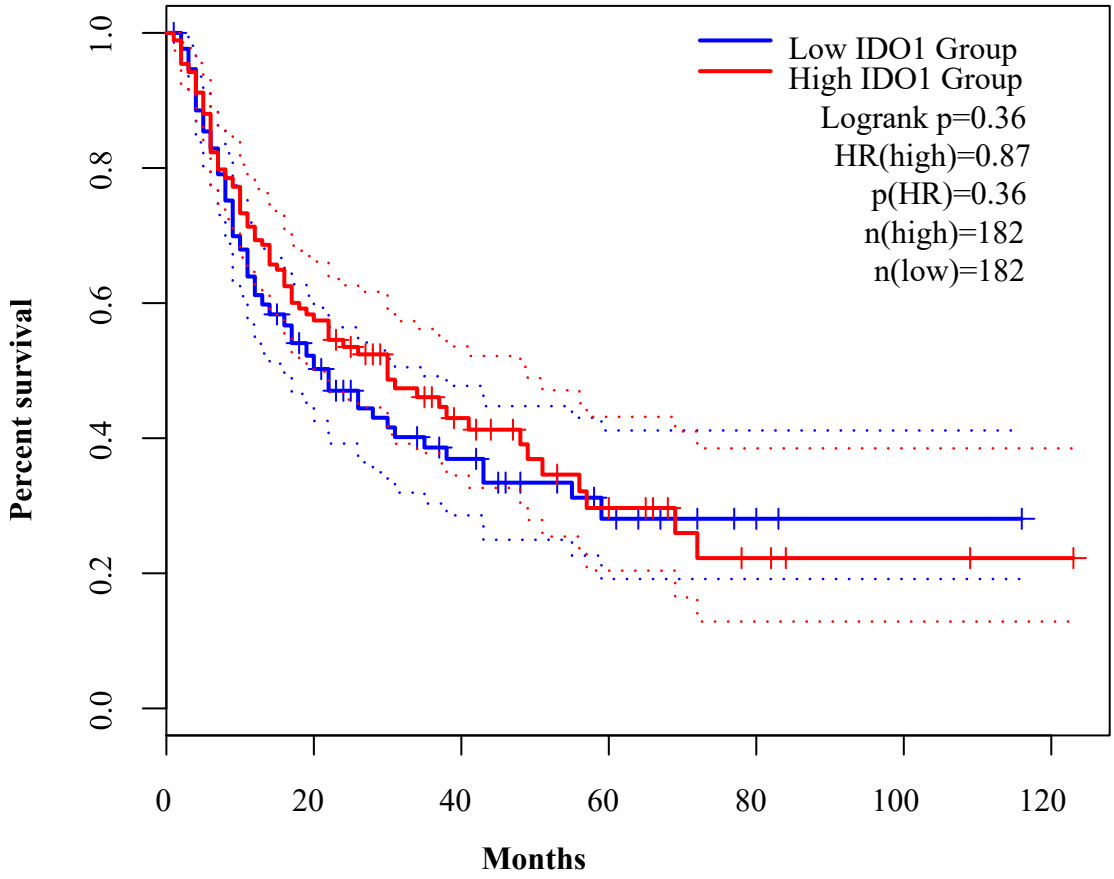


Fig 4.13: Disease Free Survival Overall data analysis, retrieved from GEPIA2: Blue line represents the group having low IDO1 expression, red line represents the group having high IDO1 expression, and blue and red dotted lines show the 95% confidence intervals for each group. X-axis represents the follow-up duration in months (time), whereas Y-axis represents the survival probability of patients (percent survival), starting at 100% and decreasing over time.

4.4.2. Association Between IDO1 Expression And Probability In LIHC Patients Through R2 Platform:

The plots retrieved through R2 platform from two different cohorts namely Tumor Liver Hepatocellular Carcinoma and Mixed Liver Hepatocellular Carcinoma.

The plot analysed the data of two factors namely gene expression and clinical variable on overall survival over the follow-up period. The p-value indicate that there is no statistically significant difference between both variables and survival outcomes (fig: 4.14).

The plot retrieved through R2 platform analysed the data of two factors namely gene expression and clinical variable on overall survival over the follow-up period. The p-value = 0.288 suggests that there is no statistically significant difference between both

variables and survival outcomes in this cohort (fig: 4.15).

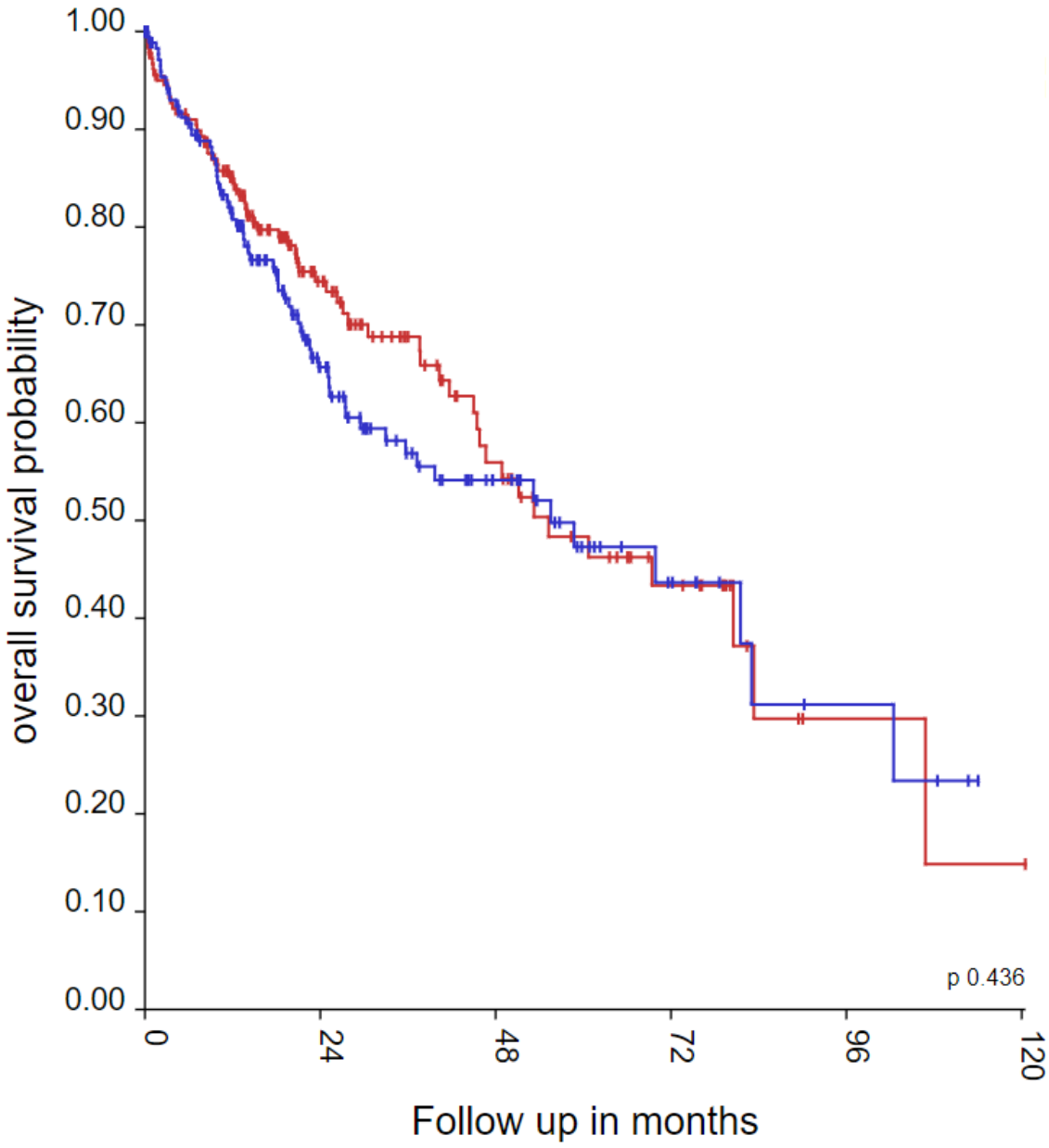


Fig:4.14: Overall survival data retrieved from (Tumor Liver Hepatocellular Carcinoma - TCGA - 371 - rsem – tcgars) dataset using R2 (genomic analysis and visualization) platform. The Kaplan–Meier survival plot, generated using patient gene expression and clinical variables, shows no statistically significant difference between the groups ($p = 0.288$), indicating that IDO1 expression alone may not strongly influence survival in this cohort.

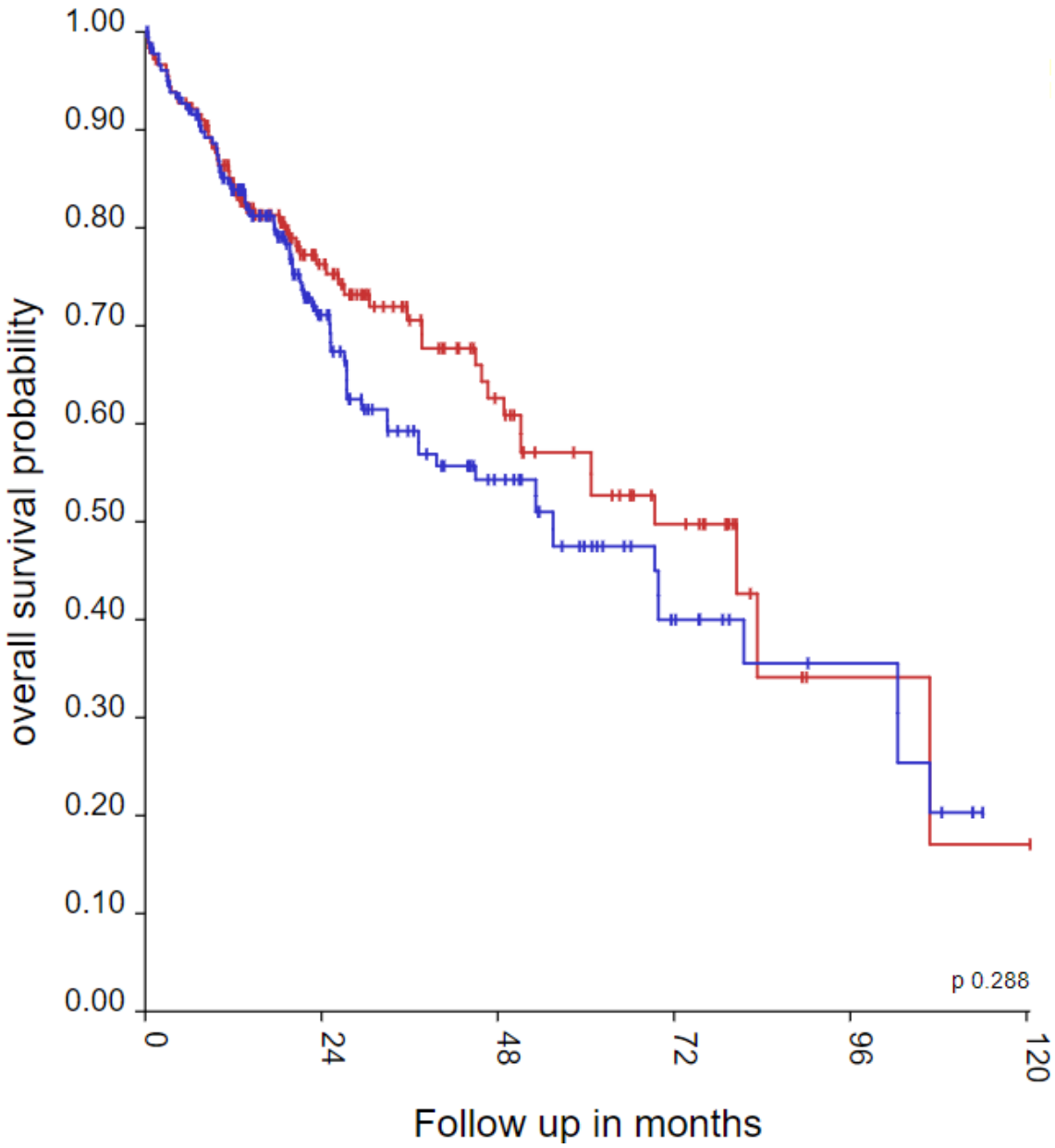


Fig: 4.15: Overall survival data retrieved from (Mixed Liver Hepatocellular Carcinoma (2022-v32) - tcga - 424 - tpm - gencode36) dataset using R2 (genomic analysis and visualization) platform. The plot compares patient groups based on IDO1 expression and clinical variables, showing a non-significant p-value (p = 0.288), suggesting no meaningful difference in survival probability between the groups in this dataset.

4.4.3. Overall Survival Data Analysis Through OncoLnc Server:

The overall survival plot was retrieved through OncoLnc server. In initial stages both groups (patients with low IDO1 expression and with high IDO1 expression) shows similar survival rates but the group with high IDO1 expression may experience better

survival outcomes than the patients with low IDO1 expression over time (fig: 4.16).

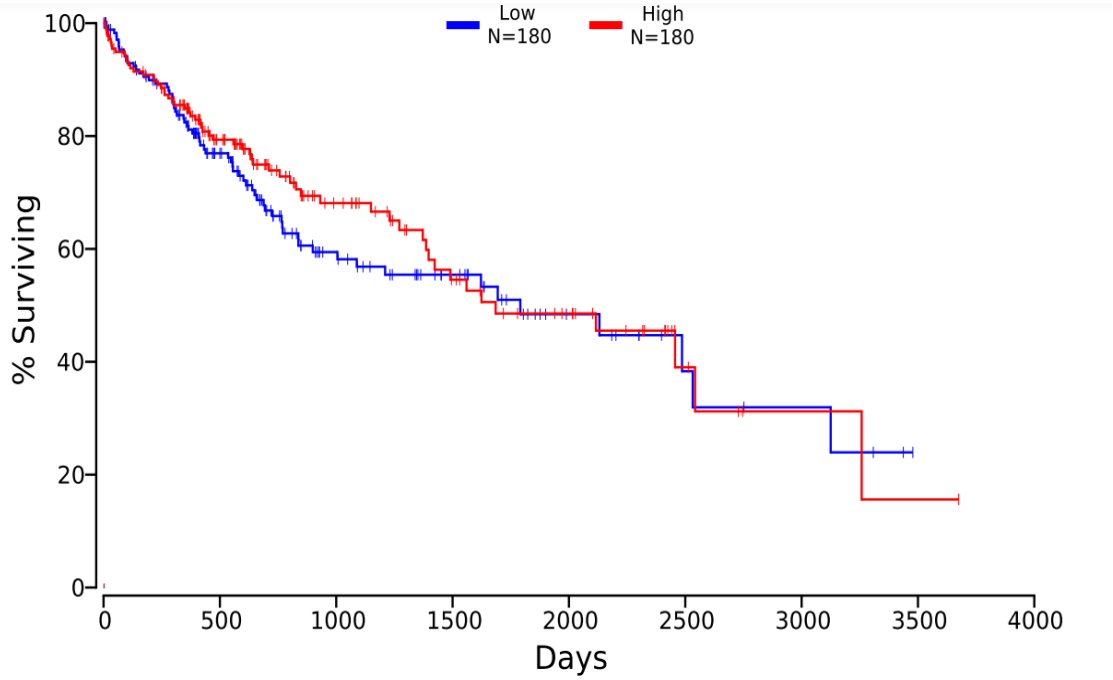


Fig:4.16: Overall survival probability of LIHC patients based on IDO1 expression levels, retrieved from the OncoLnc server. The Kaplan–Meier plot compares patients with low IDO1 expression versus those with high IDO1 expression. In the early follow-up period, both groups exhibit similar survival probabilities; however, over time, the high-IDO1 expression group trends toward slightly better survival outcomes compared to the low-expression group.

4.5. Co-Expression Analysis Of IDO1 In LIHC

4.5.1. Positively Correlated Genes With IDO Using UALCAN:

The positively correlated genes with IDO1 in LIHC were obtained from UALCAN to identify the coexpressed genes. A heatmap shows the 24 positively correlated genes with IDO1 in LIHC (fig: 4.17). Among these, the HLA-DOB gene showed the strongest co-expression with IDO1. The detailed correlation values of these 24 genes are given in Table 4.1. As shown, HLA-DOB exhibited the highest correlation with IDO1, with a Pearson correlation coefficient of 0.78, suggesting a strong positive association.

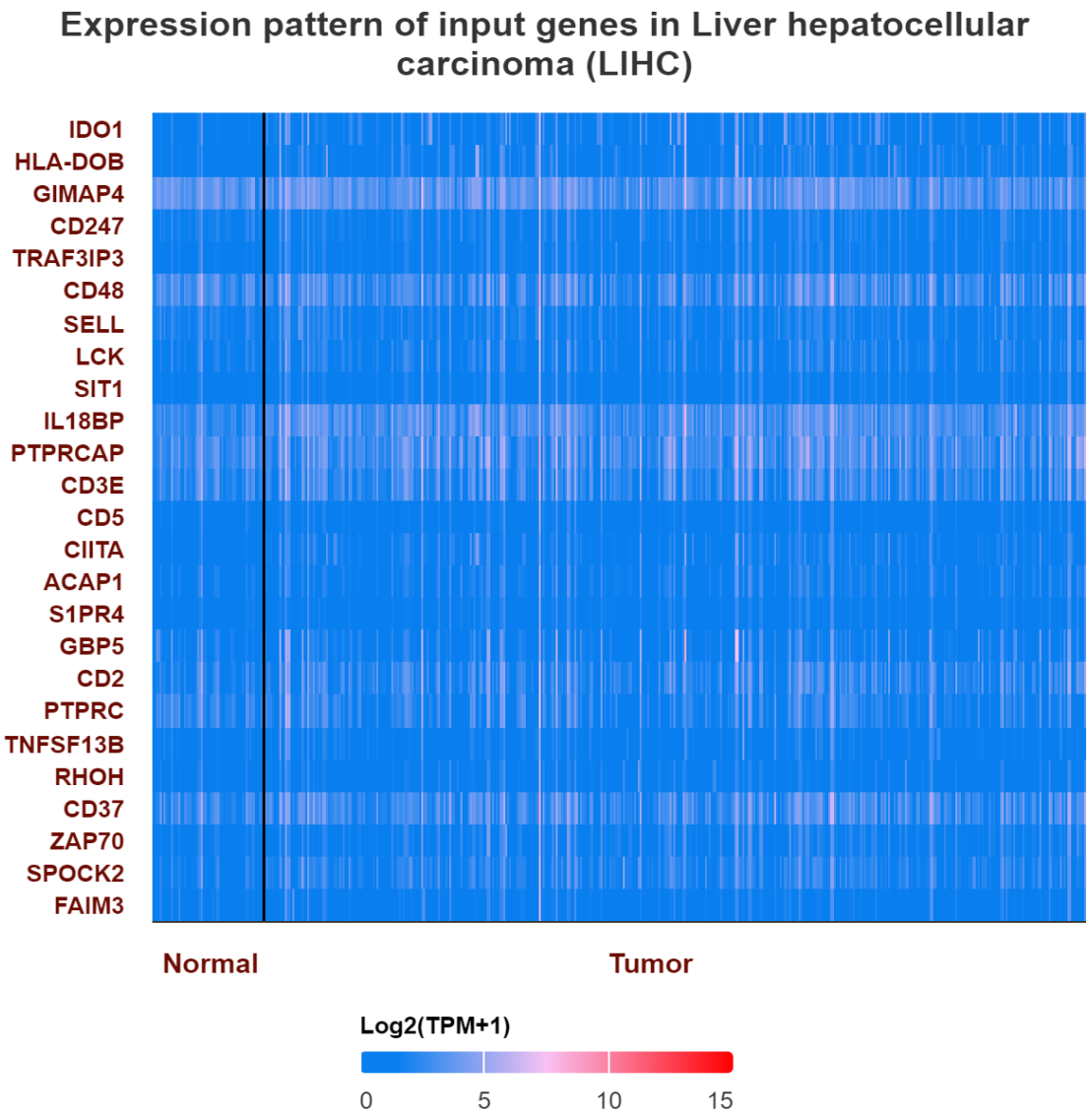


Fig: 4.17: Heatmap representing the positively correlated genes with IDO1 in LIHC, analyzed using UALCAN. A heatmap shows the 24 positively correlated genes with IDO1 in LIHC. The heatmap indicates that HLA-DOB gene was strongly co-expressed with IDO1.

Table 4.1: Positive correlated genes with IDO1 in LIHC: Table representing the positively correlated genes with IDO1 in LIHC, analyzed using UALCAN. The table indicates that HLA-DOB gene was strongly co-expressed with IDO1.

Sr no:	Genes	Pearson-CC
1	HLA-DOB	0.78
2	GIMAP4	0.72
3	CD247	0.71
4	TRAF3IP3	0.71
5	CD48	0.71
6	SELL	0.7
7	LCK	0.7
8	SIT1	0.7
9	IL18BP	0.7
10	PTPRCAP	0.7
11	CD3E	0.7
12	CD5	0.69
13	CIITA	0.69
14	ACAP1	0.69
15	S1PR4	0.69
16	GBP5	0.69
17	CD2	0.69
18	PTPRC	0.68
19	TNFSF13B	0.68
20	RHOH	0.68
21	CD37	0.68
22	ZAP70	0.68
23	SPOCK2	0.68
24	FAIM3	0.68

4.5.2. Correlation Analysis Between IDO1 And HLA-DOB:

Gene expression data for IDO1 and HLA-DOB in LIHC were retrieved from the TCGA dataset through UCSC Xena (University of California, Santa Cruz Xena browser) platform. A correlation analysis was performed, and a scatter plot was constructed using ggplot2 package in RStudio to visualize the results. The plot shows a positive correlation between IDO1 and HLA-DOB, with a Pearson correlation coefficient of 0.5195 and a Spearman correlation coefficient of 0.5022 (fig: 4.18).

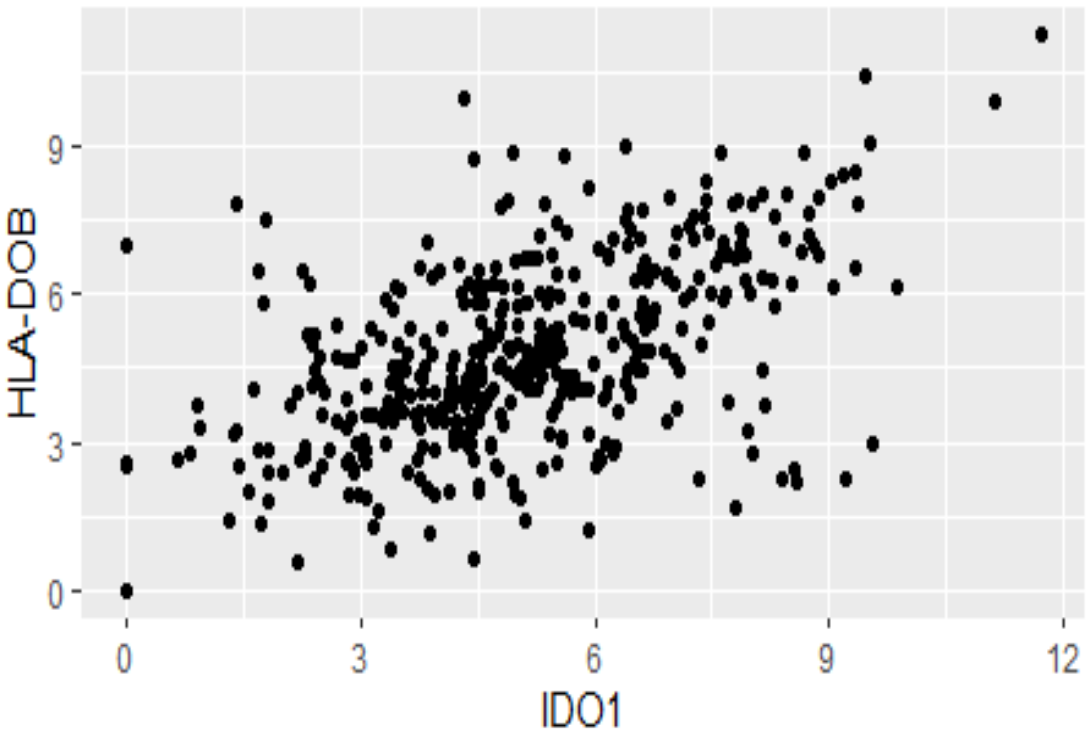


Fig: 4.18: Correlation analysis between IDO1 and HLA-DOB gene expression in Liver Hepatocellular Carcinoma (LIHC). Data were retrieved from the UCSC Xena(University of California, Santa Cruz Xena browser) platform (TCGA LIHC dataset) and analyzed in RStudio using the ggplot2 package. The unit of description is log2(norm_count+1). A moderate positive correlation was observed, with Pearson's correlation coefficient r = 0.5195 and Spearman's correlation coefficient ρ = 0.5022, indicating that higher IDO1 expression is associated with higher HLA-DOB expression in LIHC samples.

4.5.3. Correlation Analysis Between IDO1 And HLA-DOB Using GEPIA2:

The graph was generated through GEPIA2 to confirm the positive correlation between IDO1 and HLA-DOB. The plot confirmed the strong positive correlation between IDO1 and HLA-DOB, with Pearson correlated coefficient of 0.81 (fig: 4.19). It indicates that both genes may have co-regulated role in LIHC.

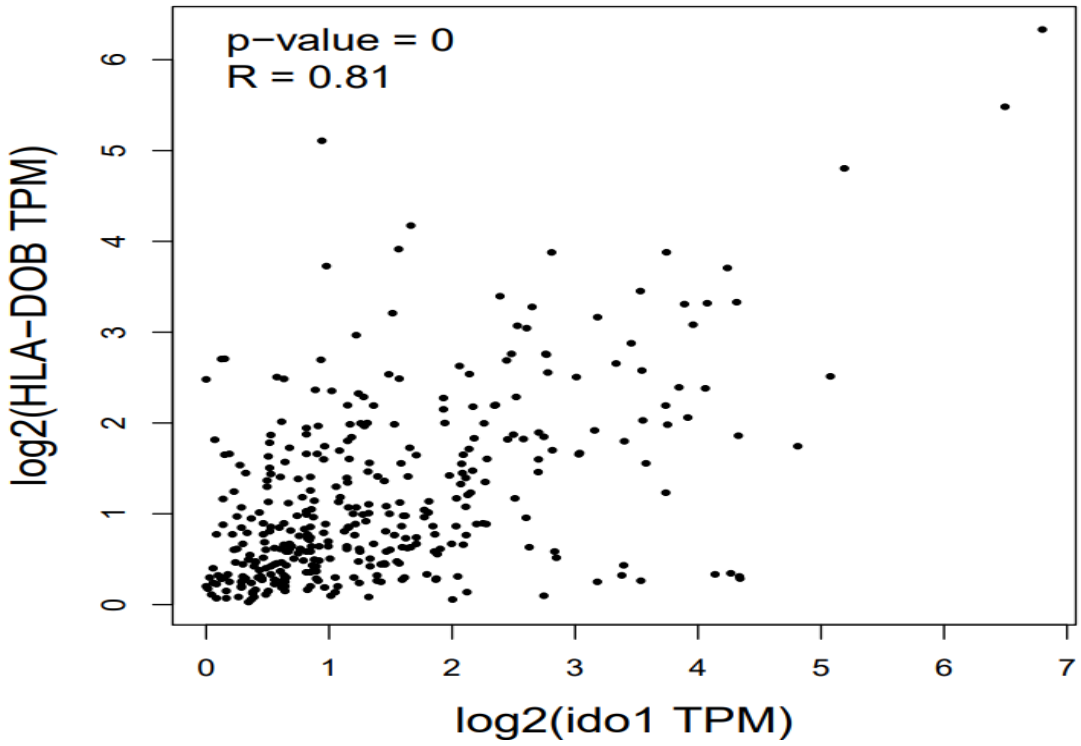


Fig: 4.19: Coexpression analysis of IDO1 and HLA-DOB expression in LIHC tumor was performed using the GEPIA2 platform (TCGA dataset). Pearson's correlation coefficient (r =0.81) indicated a strong positive relationship, suggesting that these genes may be co-regulated and potentially involved in shared molecular pathways influencing liver cancer progression.

4.6. Enrichment Analysis Of IDO1

Significantly enriched pathways of IDO1 were retrieved through Enrichr tool from five databases (table 4.2 to 4.6).

1. In reactome, the pathways related to Tryptophan Catabolism and Metabolism Of Amino Acids And Derivatives were observed (table 4.2).
2. In bioplanet, the enriched pathways were Tryptophan catabolism and metabolism, Thymic stromal lymphopoietin pathway, TGF-beta regulation, Amino acid metabolism, and Interleukin-5 regulation of apoptosis (table 4.3).
3. In wikipathways, the enriched pathways involved the IDO Metabolic Pathway, NAD Biosynthetic Pathways, Kynurenine Pathway And Links To Cell Senescence, Tryptophan Catabolism Leading To NAD Production, and Tryptophan Metabolism pathway (table 4.4).
4. In KEGG 2021 Human, the obsserved enriched pathway was Tryptophan Metabolism (table 4.5).

5. In elsevier, significantly enriched pathways were observed namely, pathways related to AHR Signaling in Treg Cell Activation, Kynurenine Metabolites in T-Cell Apoptosis, Kynurenine Metabolites Suppress T-Cells in Cancer Immune Escape, and AHR Signaling in Treg and Dendritic Cells Function (table 4.6).

For investigation of gene ontologies, two databases were used namely GO biological process 2025 and GO Molecular Function 2025. The GO biological process 2025 determined the following processes: Positive Regulation Of Lymphocyte Apoptotic Process, Tryptophan Catabolic and Metabolic Process, Kynurenine Metabolic Process, Positive Regulation Of T Cell Apoptotic Process, and Regulation Of T Cell Apoptotic Process (table 4.7).

In GO Molecular Function 2025, the enriched function was Oxidoreductase Activity (table 4.8).

This analysis suggested that IDO1 is centrally involved in immune and metabolic pathways.

Table 4.2: Top Enriched BioPlanet 2019 Pathways Identified via Enrichr

Term	**p-value**	**Adjusted p-value**	**Combined Score**
Tryptophan catabolism	5.50E-04	0.003849897	150029.821
Tryptophan metabolism	0.002899953	0.010149835	116522.3189
Thymic stromal lymphopoietin (TSLP) pathway	0.004499937	0.010499854	107587.5039
Interleukin-5 regulation of apoptosis	0.007199916	0.012599854	97963.26643
Amino acid metabolism	0.0097499	0.01364986	91707.01721
TGF-beta regulation of extracellular matrix	0.028249829	0.032958133	69318.19039
Metabolism	0.080749756	0.080749756	46264.02018

Table 4.3: Top Enriched KEGG Pathways 2021 Human Identified via Enrichr

Term	**p-value**	**Adjusted p-value**	**Combined Score**
African trypanosomiasis	0.00185	0.002099962	125618.9446
Tryptophan metabolism	0.0021	0.002099962	123057.7561

Table 4.4: Top Enriched Reactome Pathways 2024 Identified via Enrichr

Term	p-value	Adjusted p-value	Combined Score
Tryptophan Catabolism	7.00E-04	0.002099947	145187.4054
Metabolism of Amino Acids and Derivatives	0.0179	0.026849793	79019.02517
Metabolism	0.10905	0.109049745	39486.03315

Table 4.5: Top Enriched WikiPathways 2024 Human Identified via Enrichr

Term	p-value	Adjusted p-value	Combined Score
IDO Metabolic Pathway WP5414	5.50E-04	0.002399948	150029.821
Tryptophan Catabolism Leading To NAD Production WP4210	8.00E-04	0.002399948	142504.3668
NAD Biosynthetic Pathways WP3645	0.001099976	0.002399948	136099.4703
Kynurenine Pathway And Links To Cell Senescence WP5044	0.001199974	0.002399948	134347.6949
Tryptophan Metabolism WP465	0.001649968	0.002639948	127928.5603
T Cell Modulation In Pancreatic Cancer WP5078	0.00229996	0.003066613	121217.8313
ADHD And Autism ASD Pathways WP5420	0.01849986	0.021142697	78323.54567
Pleural Mesothelioma WP5087	0.021849848	0.021849848	74800.33027

Table 4.6: Top Enriched Elsevier Pathways Identified via Enrichr

Term	p-value	Adjusted p-value	Combined Score
Kynurenine/AHR Signaling in Treg Cell Activation	2.00E-04	0.002159943	170310.4867
Kynurenine Metabolites in Neurotoxicity and Neuroprotection	5.50E-04	0.002159943	150029.821
Aryl Hydrocarbon Receptor/Tryptophan Metabolites Signaling	5.50E-04	0.002159943	150029.821
Kynurenine Metabolites in T-Cell Apoptosis	6.00E-04	0.002159943	148283.1196

Kynurenine Metabolites Supress T-Cells in Cancer Immune Escape	6.00E-04	0.002159943	148283.1196
AHR Signaling in Treg and Dendritic Cells Function	0.00115	0.003449925	135204.6392
Tumor Infiltrating Macrophages in Cancer Progression and Immune Escape	0.0018	0.004162421	126172.2336
Plasmacytoid Dendritic Cell in Diabetes Mellitus Type 1	0.00185	0.004162421	125618.9446
Proteins with Altered Expression in Cancer Immune Escape	0.0024	0.004799917	120356.5273
Proteins Involved in Diffuse Large-B-Cell Lymphoma	0.00305	0.005154464	115499.2434

Table 4.7: Top Enriched Biological Processes (GO-BP) 2025 for IDO1 via Enrichr

Term	**p-value**	**Adjusted p-value**	**Combined Score**
Positive Regulation of Lymphocyte Apoptotic Process (GO:0070230)	3.50E-04	8.57E-04	159096.4487
L-tryptophan Catabolic Process (GO:0006569)	3.50E-04	8.57E-04	159096.4487
L-tryptophan Metabolic Process (GO:0006568)	3.50E-04	8.57E-04	159096.4487
Kynurenine Metabolic Process (GO:0070189)	4.00E-04	8.57E-04	156418.9114
Erythrose 4-Phosphate/Phosphoenolpyruvate Family Amino Acid Catabolic Process (GO:1902222)	5.00E-04	8.57E-04	151942.5909
Positive Regulation of T Cell Apoptotic Process (GO:0070234)	5.50E-04	8.57E-04	150029.821
Regulation of T Cell Apoptotic Process (GO:0070232)	6.00E-04	8.57E-04	148283.1196
Aromatic Amino Acid Family Catabolic Process (GO:0009074)	8.50E-04	0.00106247	141285.7658
Regulation of Activated T Cell Proliferation (GO:0046006)	0.00165	0.001833297	127928.5603
Regulation of T Cell Proliferation (GO:0042129)	0.00415	0.00414994	109237.9989

Table 4.8: Top Enriched Molecular Function (GO-MF) 2025 for IDO1 via Enrichr

Term	p-value	Adjusted p-value	Combined Score
Oxidoreductase, Single Donors W Incorp of O2, Incorp of Two Atoms of O (GO:0016702)	0.0011	0.001099976	136099.4703

4.7. Evaluation Of IDO1 Interaction Network

4.7.1. Protein-Protein Interaction Using STRING Database:

The protein-protein interaction of IDO1 were retrieved through STRING (Search Tool for the Retrieval of Interacting Genes/Proteins) database. The interaction network showed the interaction of IDO1 with CYP1A1, CYP1B1, AFMID, TDO2, IL4I1, KYNU, TPH1, TPH2, MAOA, and MAOB (fig: 4.20). Table 9 showed that TDO2 is a highly confident predicted functional partner of IDO1, exhibiting high interaction score of 0.990.

The network analysis indicates a highly interconnected system with following information:

Number of nodes: 11

Number of edges: 37

Average node degree: 6.73

Avg. Local clustering coefficient: 0.854

Expected number of edges: 11

PPI enrichment p-value: 2.49e-10

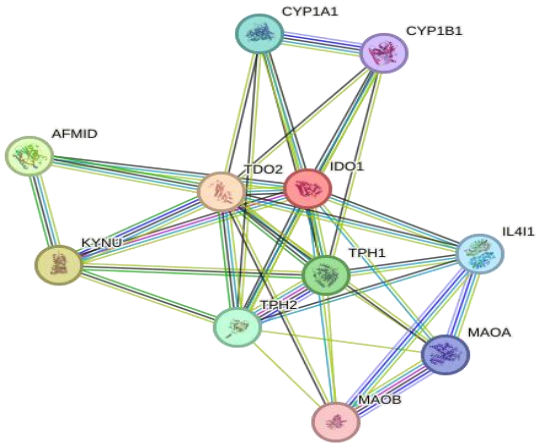


Fig 4.20: IDO1 interacting network of proteins, retrieved from STRING (Search Tool for the Retrieval of Interacting Genes/Proteins) tool.

Table 9: Top Functional Partner Proteins of IDO1

Predicted functional partners	**Scores (Confidence level) 0-1**
Tryptophan 2,3-dioxygenase (TDO2)	0.990
Kynureninease (KYNU)	0.983
Kynurenine formamidase (AFMID)	0.968
Tryptophan hydroxylase 1 (TPH1)	0.957
Tryptophan hydroxylase 2 (TPH2)	0.953
Cytochrome P450 1A1 (CYP1A1)	0.944
L-amino acid oxydase (IL4I1)	0.941
Amine oxydase [flavin-containing] A (MAOA)	0.939
Cytochrome P450 1B1 (CYP1B1)	0.938
Amine oxydase [flavin-containg] B (MAOB)	0.936

4.7.2. IDO1 Interaction Network Using Genemania:

The IDO1-gene and protein interaction network was obtained through GeneMANIA. The network shows predicted and experimentally validated interactions of IDO1 with multiple genes. It revealed the interaction of IDO1 with AFMID, IDO2, TDO2, BIN1, AGXT, PPP1R16A, DDX244, AMT, MTHFD1, SHMT2, GPT, IMMP2L, PTPN6, CXCL9, SHMT1, CXCL11, SOCS3, RBKS, TERF2IP, and CXCL10. The analysis revealed strong co-expression and pathway-based interactions with AFMID, IDO2, and TDO2, reflecting their shared role in tryptophan metabolism.

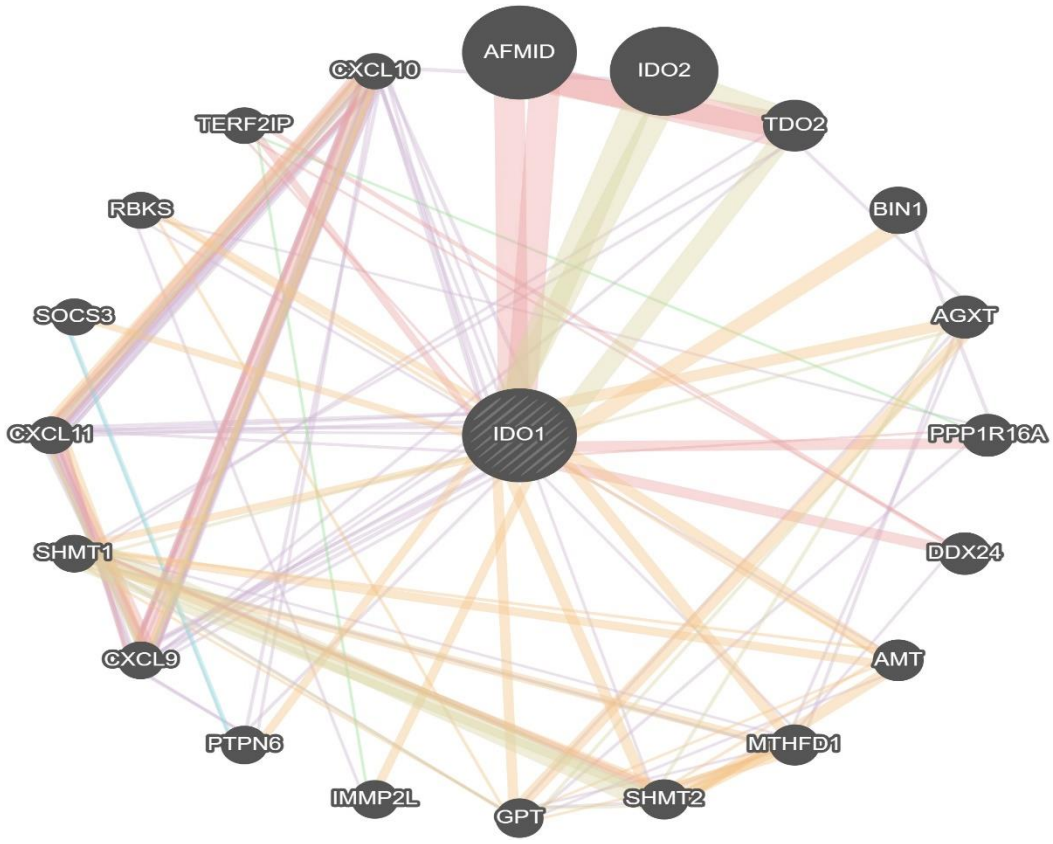


Fig 4.21: The IDO1-gene and protein interaction network was obtained through GeneMANIA. The network shows predicted and experimentally validated interactions of IDO1 with multiple genes. The analysis revealed strong co-expression and pathway-based interactions with AFMID, IDO2, and TDO2, reflecting their shared role in tryptophan metabolism.

4.8. Network Analysis Of IDO1 Using Network Analyst:

4.8.1. Transcription Factor (TF) Analysis:

The IDO1-interacting transcription factors were obtained by Network Analyst platform. Table 4.9 suggests that IDO1 is potentially regulated by various TFs, including: STAT3, PRDM14, MYC, SMARCA4, ASH2L, BACH1, EOMES, FOXA1, TP53, RELA, SMAD3, ATF3, RNF2, SALL4, and AR. The regulators may show the regulatory influences in development, immune modulation, and cell differentiation.

Table 4.9: IDO1-interacting transcription factors (immune-related TFs highlighted in blue)

Sr. No.	Transcription Factor (Abbreviation)	Possible Functional Role
1	AR	Hormone-dependent gene regulation; potential modulation of immune-related genes
2	STAT3	Regulates immune responses, inflammation, and oncogenesis
3	MYC	Cell proliferation, metabolism, and tumorigenesis
4	TP53	Tumor suppression, apoptosis regulation
5	ASH2L	Epigenetic regulation, chromatin remodeling
6	EOMES	Regulation of T-cell differentiation, immune modulation
7	SMARCA4	Chromatin remodeling, transcriptional regulation
8	SALL4	Stem cell maintenance, developmental regulation
9	PRDM14	Stemness maintenance, epigenetic gene regulation
10	ATF3	Stress response, apoptosis, immune regulation
11	SMAD3	TGF-β signaling, immune regulation, fibrosis
12	RNF2	Histone modification, transcription repression
13	RELA	Inflammatory response, immune activation
14	BACH1	Oxidative stress response, heme metabolism regulation
15	FOXA1	Hormone receptor regulation, epithelial differentiation

4.8.2. miRNA Network Analysis Of IDO1:

The miRNAs interacted with IDO1 were retrieved from TarBase data base using NetworkAnalyst platform. The analysis indicates the direct interaction of 20 miRNA with IDO1. It may modify the expression of IDO1 at the posttranscriptional stage(table 4.10).

Table 4.10: miRNAs interacting with IDO1 as identified through TarBase (NetworkAnalyst)

miRNA	Known Role / Function
hsa-miR-19a-3p	Regulates immune checkpoint pathways; promotes tumor progression
hsa-miR-19b-3p	Modulates inflammatory cytokines; involved in oncogenesis
hsa-miR-25-3p	Suppresses apoptosis; modulates TGF-β pathway
hsa-miR-27a-3p	Influences angiogenesis, tumor invasion
hsa-miR-196a-5p	Associated with epithelial-mesenchymal transition (EMT)
hsa-miR-34a-5p	p53 target; regulates T-cell activation and apoptosis
hsa-miR-200b-3p	Controls EMT and immune suppression
hsa-miR-130a-3p	Alters macrophage polarization; angiogenesis
hsa-miR-133a-3p	Inhibits tumor cell proliferation and migration
hsa-miR-194-5p	Tumor suppressor; regulates inflammation
hsa-miR-200c-3p	EMT regulator; modulates PD-L1 expression
hsa-miR-302a-3p	Involved in stemness and cell cycle control
hsa-miR-34b-5p	p53 pathway; immune activation
hsa-miR-34c-5p	Apoptosis induction; T-cell modulation
hsa-miR-373-3p	Enhances tumor metastasis
hsa-miR-449a	Regulates cell cycle; suppresses immune evasion
hsa-miR-452-5p	EMT regulation; tumor invasion
hsa-miR-92b-3p	Promotes cancer cell proliferation
hsa-miR-449b-5p	Cell cycle arrest; immune modulation
hsa-miR-129-2-3p	Tumor suppressor activity

*Highlighted miRNAs are strongly linked to immune modulation and cancer progression, directly relevant to IDO1 regulation.

4.9: Quantum Analysis Of Active Site Of IDO1 Using Density Functional Theory DFT:

Density Functional Theory (DFT) calculations were performed to investigate the electronic and structural properties of the IDO1 active site. The model system included the heme prosthetic group, cyanide ligand, and tryptophan substrate that are directly involved in catalytic activity. The B3LYP functional with the DEF2-SVP basis set was employed for geometry optimization and electronic property analysis. Solvent effects were incorporated using CPCM and SMD solvation models to mimic the enzyme's aqueous environment (fig 4.22).

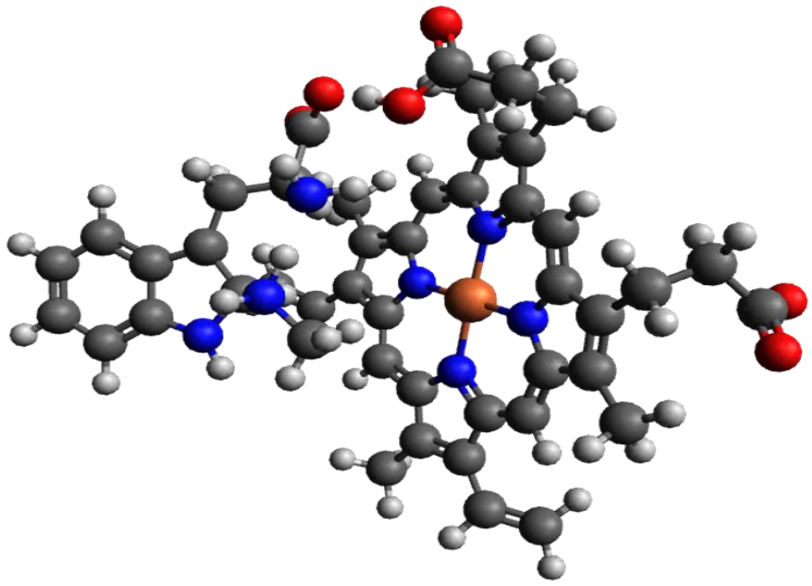


Figure 4.22: Optimized geometry of the IDO1 active site obtained using ORCA 6.0 software. The model system includes the heme prosthetic group, Fe(III) center, cyanide ligand, and bound tryptophan substrate. DFT calculations were performed at the B3LYP/DEF2-SVP level of theory with CPCM and SMD solvation models to mimic the aqueous enzyme environment. The structure illustrates the coordination of Fe(III) with porphyrin nitrogens and the positioning of the substrate within the catalytic pocket, highlighting the electronic and structural features relevant to IDO1's catalytic activity.

The HOMO-LUMO energy gap of the active site was calculated as 1.33 eV, suggesting a moderately reactive electronic environment. This gap is consistent with the redox activity typically required for oxygen incorporation into substrates, as occurs during the oxidation of tryptophan to N-formylkynurenine by IDO1.

The Mayer bond order analysis revealed that the iron atom of the heme group maintained typical Fe–N coordination with the porphyrin nitrogens, with bond orders ranging from 0.6910 to 0.7035. This result confirms the structural integrity of the catalytic iron center. Additionally, carbonyl bond orders such as C(11)-O(12) at 1.9808, and C(35)-O(36) at 1.8420, indicate strong double-bond character, suggesting stabilization of substrate intermediates. The observed O–H interactions, including O(13)-H(106) at 0.7659, reflect potential hydrogen bonding within the active site, relevant for proton transfer during catalysis.

Hydrocarbon bond orders within the heme macrocycle and active site side chains were in the range of 1.3 to 1.5, indicating delocalized π-systems, while some C–C bond

orders approached 1.9, highlighting conjugation patterns crucial for maintaining the heme pocket's structural rigidity.

The spin population analysis confirmed that the system adopts a high-spin Fe(III) state, with the majority of unpaired electrons localized on the iron atom's d-orbitals (2.6879 spin density). Nitrogen atoms of the porphyrin ring also exhibited minor but significant spin contributions (e.g., N38: -0.0309, N40: -0.0319), indicative of spin delocalization due to Fe–N interactions. The total spin multiplicity corresponded to S = 2 (quartet state), consistent with biologically relevant IDO1 oxidation states. The total electronic energy was calculated as -3875.786 Eh, with a nuclear repulsion energy of +10019.55 Eh, and electronic stabilization energy of -13895.08 Eh. The virial ratio of 2.007 confirmed the physical validity of the calculation.

4.10: Molecular Docking Of IDO1 With Ligand Quercetin:

Molecular docking of IDO1 with Quercetin was performed using AutoDock Vina in PyRx. IDO1 was docked with ligand Quercetin. The docked pose reveals the binding site of Quercetin within IDO1's active pocket, showing the orientation and stability of interaction. It provides insights into Quercetin's potential role as an IDO1 inhibitor, supporting its relevance in cancer biomarker and therapeutic studies (fig 4.23).

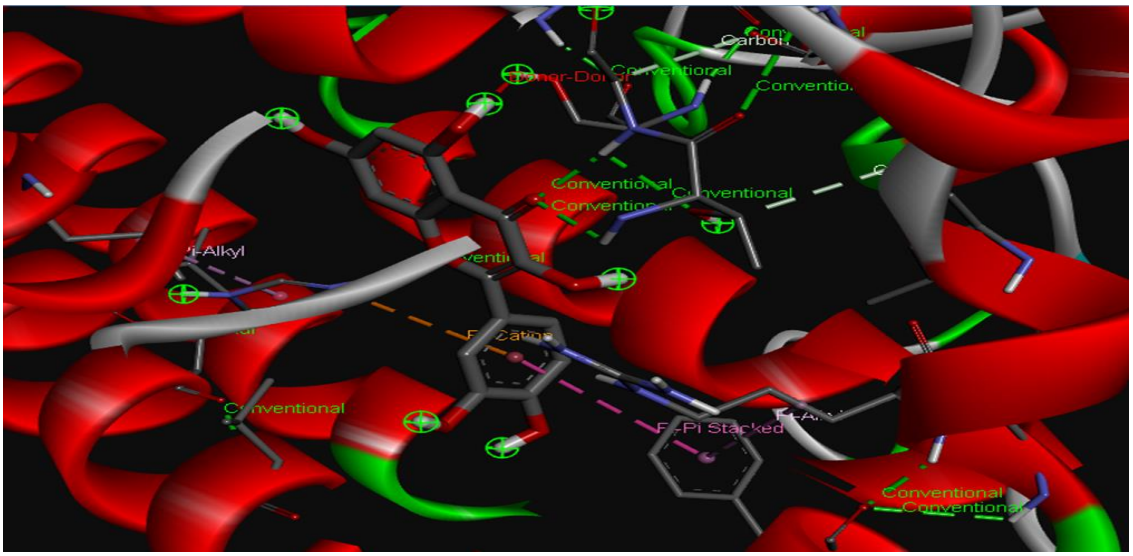


Fig 4.23: (a) The docked pose of IDO1protein with Quercetin ligand: Molecular docking of IDO1 with Quercetin was performed using AutoDock Vina in PyRx. The docked pose reveals the binding site of Quercetin within IDO1's active pocket, showing the orientation and stability of interaction. It provides insights into Quercetin's potential role as an IDO1 inhibitor, supporting its relevance in cancer biomarker and therapeutic studies.

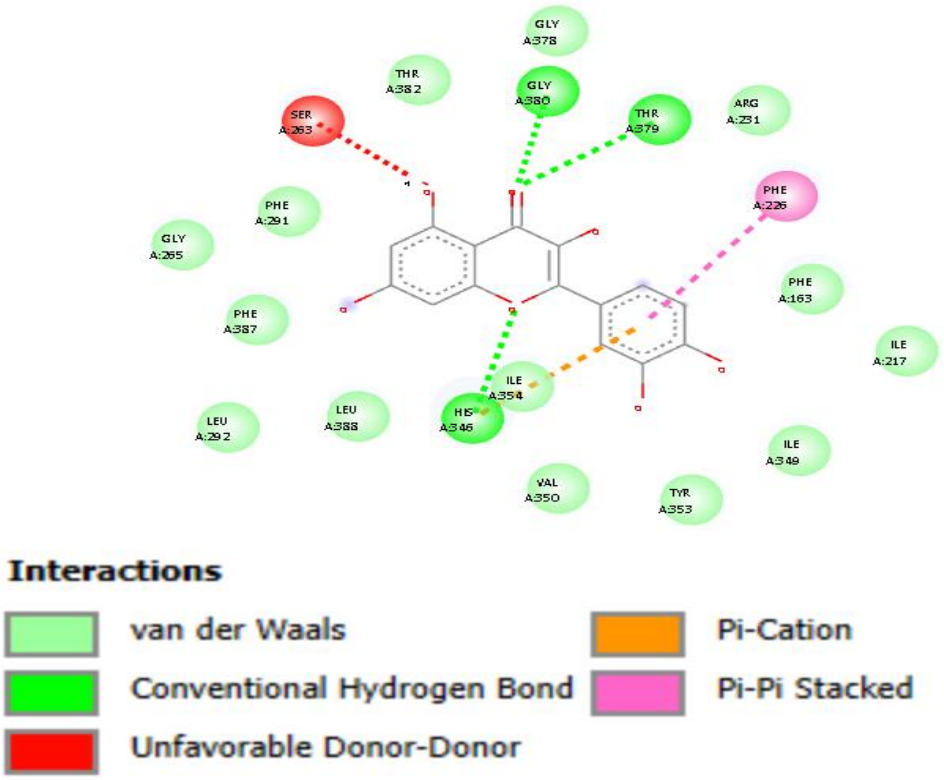


Fig 4.23: (b) 2D representation of protein and ligand interaction. It shows the formation of conventaional hydrogen bond between the O group of ligand and His 346, Thr 379 and Gly 380 amino acid residues of protein. Pi-cation bond is formed between ligand and His 346 amino acid residues of protein. Pi-Pi Stacked bond is formed between ligand and Phe 226 amino acid residue of protein. Other van der waal forces indicates the close contact between protein and ligand.

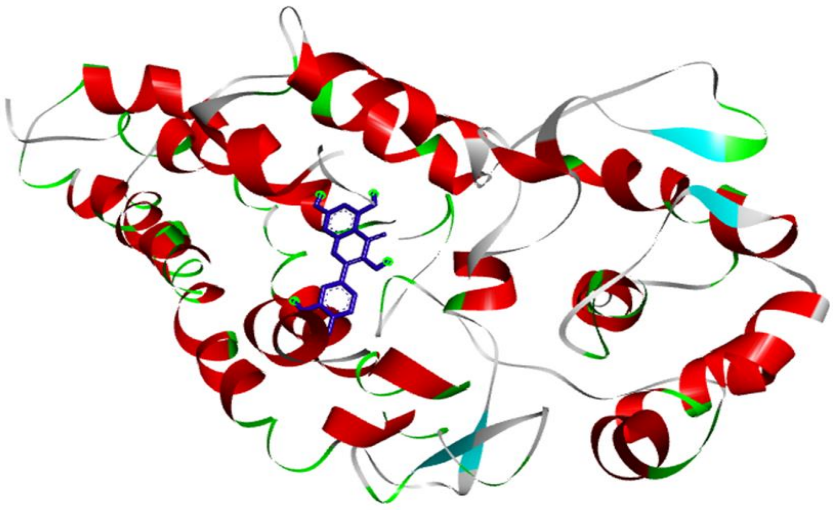


Fig 4.24: The full image of IDO1- Quercetin interaction in a 3D representation. The ligand model of quercetin attached with IDO1 protein which can be visualized in the image.

4.11. Statistical Analysis Of Gene Expression And Patient Survival In LIHC

4.11.1. Evaluation Of Diagnostic Value Of IDO1:

Expression data were retrieved from the GEO database and analyzed using the DATAtab online tool. Patient status was set as the state variable and IDO1 expression values as the test variable. The AUC for the IDO1 expression was 0.91. It indicates that IDO1 might be used as diagnostic marker (fig: 4.25).

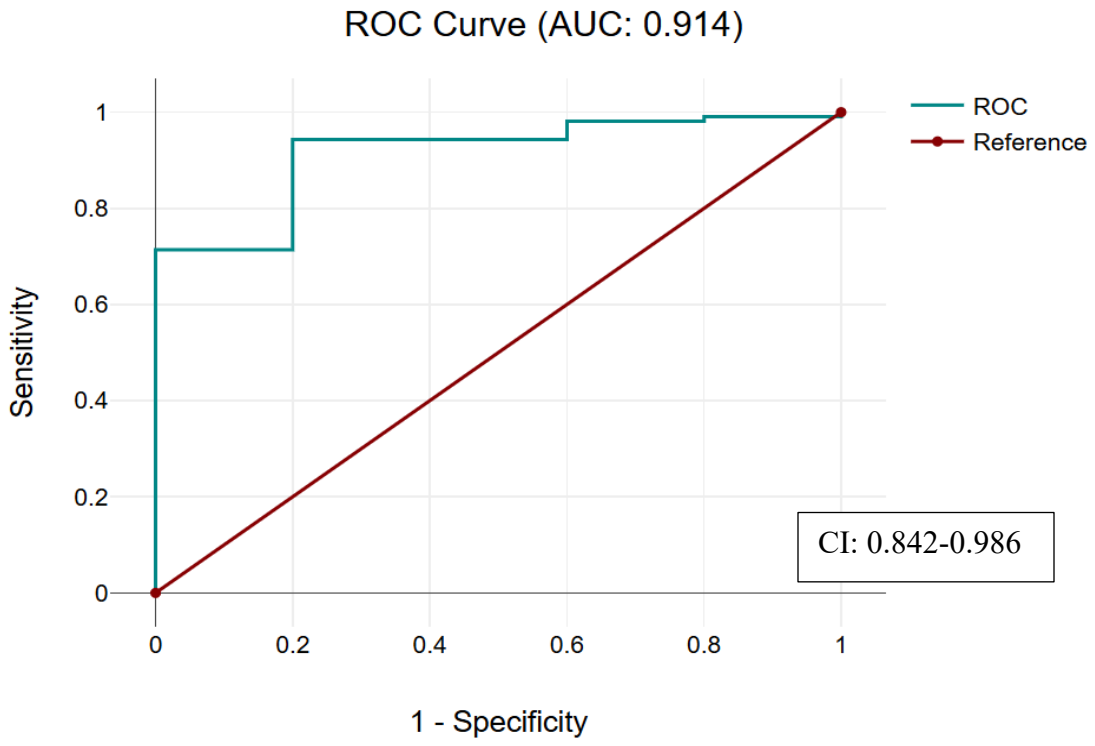


Figure 4.25: Receiver Operating Characteristic (ROC) curve for the diagnostic evaluation of IDO1 gene expression. Expression data were retrieved from the GEO database and analyzed using the DATAtab online tool. Patient status was set as the state variable and IDO1 expression values as the test variable. The AUC (Area under curve) value indicating excellent diagnostic potential. The 95% confidence interval (CI) was calculated using the DeLong method: CI = AUC ± Z × SE, where $n^+ = 423$, $n^- = 5$, and $Z \approx 1.96$.

4.11.2. Evaluation Of Prognostic Value Of IDO:

Survival data were retrieved from the OncoLnc platform (Kaplan–Meier analysis for LIHC) and analyzed using the DATAtab online tool. Patient survival status was set as the state variable and IDO1 expression values as the test variable. The AUC for the IDO1 expression was 0.51. It indicates low prognostic discrimination (fig: 4.26).

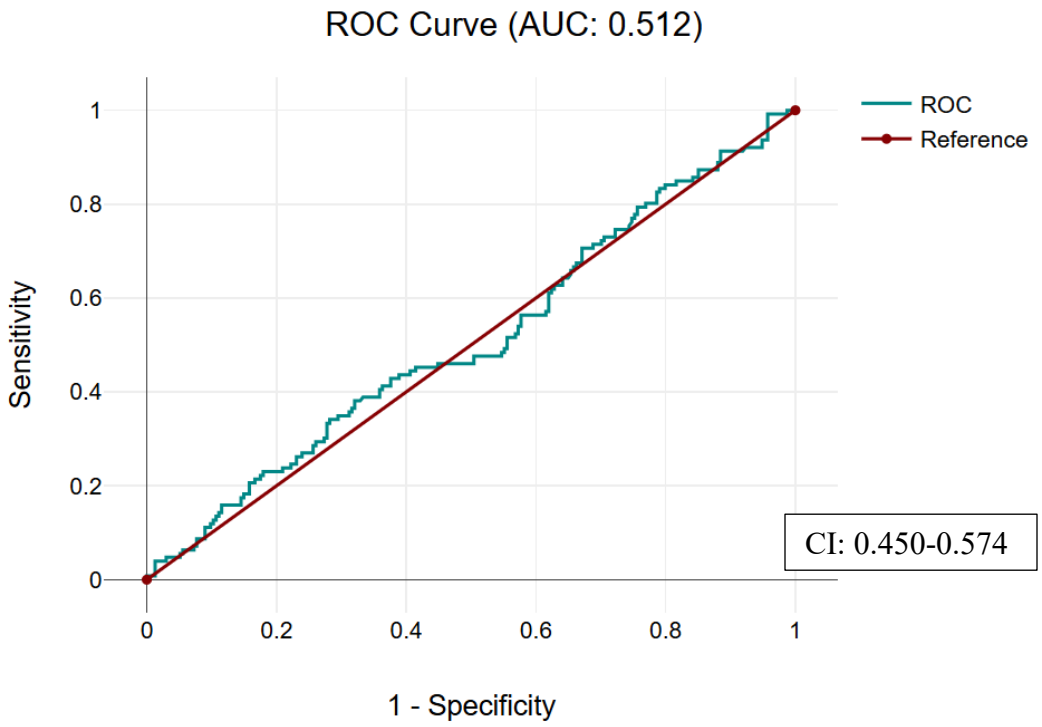


Fig 4.26: Receiver Operating Characteristic (ROC) curve for the prognostic evaluation of IDO1 gene in LIHC. Survival data were retrieved from the OncoLnc platform (Kaplan–Meier analysis for LIHC) and analyzed using the DATAtab online tool. Patient survival status was set as the state variable and IDO1 expression values as the test variable. The ROC curve showed an AUC value of 0.54, indicating low prognostic discrimination. The 95% confidence interval (CI) was calculated using the DeLong method: CI = AUC ± Z × SE, where $n^+ = 234$, $n^- = 126$, and $Z \approx 1.96$.

CHAPTER 5
DISCUSSION

Liver cancer, especially hepatocellular carcinoma (LIHC), is one of the leading causes of cancer-related mortality worldwide. Due to its asymptomatic progression, it is often diagnosed at an advanced stage, which makes early detection extremely important. According to the WHO (2024), liver cancer is the third leading cause of cancer death in the world. Liver is an immunologically unique organ, naturally designed to tolerate inflammation. This makes immune escape mechanisms -like IDO1 overexpression - even more critical in liver cancer progression. Targeting IDO1 could improve the effectiveness of immunotherapies in LIHC.

This study assessed the potential of IDO1 as a biomarker in LIHC patients through bioinformatic analyses. The mRNA expression of IDO1 in LIHC and the other carcinomas was observed via GEPIA, GENT2, and UALCAN. IDO1 is an immune-regulatory enzyme that plays a pivotal role in the conversion of tryptophan-kynurenine and it also promotes immune tolerance within the tumor microenvironment by depleting tryptophan and generating immunosuppressive metabolites [46].

The GEPIA analysis shows that IDO expression is regulated in different cancer types namely ACC (Adrenocortical Carcinoma), BLCA (Bladder Urothelial Carcinoma), BRCA (Breast Invasive Carcinoma), CESC (Cervical Squamous Cell Carcinoma and Endocervical Adenocarcinoma), CHOL (Cholangiocarcinoma), COAD (Colon Adenocarcinoma), DLBC (Lymphoid Neoplasm Diffuse Large B-cell Lymphoma), ESCA (Esophageal Carcinoma), GBM (Glioblastoma Multiforme), HNSC (Head and Neck Squamous Cell Carcinoma), KICH (Kidney Chromophobe), KIRC (Kidney Renal Clear Cell Carcinoma), KIRP (Kidney Renal Papillary Cell Carcinoma), LIHC (Liver Hepatocellular Carcinoma), LUAD (Lung Adenocarcinoma), LUSC (Lung Squamous Cell Carcinoma), OV (Ovarian Serous Cystadenocarcinoma), PAAD (Pancreatic Adenocarcinoma), PCPG (Pheochromocytoma and Paraganglioma), PRAD (Prostate Adenocarcinoma), READ (Rectum Adenocarcinoma), SARC (Sarcoma), SKCM (Skin Cutaneous Melanoma), STAD (Stomach Adenocarcinoma), TGCT (Testicular Germ Cell Tumors), THCA (Thyroid Carcinoma), THYM (Thymoma), UCEC (Uterine Corpus

Endometrial Carcinoma), and UCS (Uterine Carcinosarcoma).

Upregulated IDO1 gene expression in LIHC and other cancer types was also assessed by UALCAN and GENT2. The UALCAN analysis shows the upregulation of expression in 18 cancer types, including STAD, READ, ESCA, KIRC, LIHC, HNSC, LUAD, CHOL, PCPG, COAD, UCEC, GBM, BRCA, CESC, KIRP, KICH, SARC, and BLCA. These findings suggest a broad role of IDO1 in tumor immune escape mechanisms, consistent with previous reports showing IDO1 overexpression in various solid tumors [47]. Further validation for GENT2 revealed the upregulation in 26 cancer types, including those of the liver, adipose, lymph-node, oral, ovary, pharynx, adrenal gland, bladder, bone, skin, small intestine brain, spleen, stomach, testis, breast, cervix, colon, thyroid, tongue, uterus, esophagus, gallbladder, head and neck, vagina, vulva, and kidney. Collectively, these observations support that IDO1 is frequently activated in tumor cells, functioning as an immunological resistance mechanism against T-cell-mediated cytotoxicity [48,49].

In liver related cancers namely CHOL and LIHC, differential expression analyses using UALCAN and GEPIA2 revealed significant IDO1 upregulation compared with normal tissues. It is well established that IDO1 is involved in the immune evasion mechanisms of biliary tract cancers. Elevated IDO1 expression in cholangiocarcinoma fosters an immunosuppressive tumor microenvironment, allowing cancer cells to escape cytotoxic T-cell responses [50]. Moreover, high IDO1 activity in cholangiocarcinoma correlates with poor prognosis, largely through recruitment of regulatory T cells (Tregs) and attenuation of antitumor immunity [51]. The differential expression analysis corroborated earlier findings of IDO1's immunosuppressive role in hepatocellular carcinoma by showing significantly higher IDO1 expression in LIHC compared with normal hepatic tissue [50].

Cancer is a complex and heterogeneous disease, with gene expression level vary in different clinicopathological settings. Recognizing cancer's heterogeneity, this study analyzed IDO1 expression based on patient's race, age, tumor stage, tumor grade, and also the nodal status.

The findings indicate a significant increase in IDO1 expression from normal tissue to early and late-stage LIHC, highlighting IDO1's involvement in tumor progression and

development. However, in Stage 4 cancer, no significant difference in IDO1 levels was observed compared to normal tissue. This plateau effect suggests that IDO1 expression stabilizes in late-stage cancer, possibly due to tumor-induced immune tolerance already being fully achieved by that time [51]. The results are consistent with reported studies that IDO1 upregulation is prominent in early to intermediate stages of cancer, where it facilitates immune escape and T-cell suppression, but may not continuously increase in terminal disease stages [52].

The analysis also revealed higher IDO1 expression in both Caucasian and Asian patients. It suggests that IDO1 overexpression is not population-specific, but may reflect a universal immune-escape mechanism across different racial groups. It is reported that immune checkpoint-related pathways, including IDO1, are dysregulated across diverse populations, though the degree of expression may vary depending on genetic and environmental factors [53].

The results showed that IDO1 was highly upregulated among individuals aged 41-100 years. This may be attributed to immune senescence, a phenomenon where the immune system becomes weaker and less regulated with age, leading to increased expression of immune-suppressive factors such as IDO1. [54]. The lower expression in younger patients might indicate a more robust immune response or less reliance on IDO1-mediated immune escape in early-onset liver cancers.

The nodal metastasis results revealed that the IDO1 expression shows a statistically significant difference in tumors without lymph node involvement (N0), when compared to normal group. On the other hand, N1 do not show significant results. However, the expression of IDO1 is significantly higher in N1 as compared to N0 patients, suggesting its importance as a cancer biomarker for lymphatic involvement in LIHC. This trend suggests that IDO1 may play a role in early tumor spread but its expression levels do not necessarily increase linearly with nodal metastasis, possibly due to complex tumor-immune interactions during metastasis [55].

Based on tumor grade, the findings show an increase in IDO1 expression in Grades 1, 2, and 3 tumors compared to normal tissues, indicating that IDO1 may play a role in early to intermediate cancer stages. This pattern implies that IDO1 may contribute to the establishment of an immunosuppressive tumor microenvironment at initial stages, thereby

facilitating tumor progression. These findings align with those of Huang et al. (2020), who demonstrated that IDO1 expression increases from low- to intermediate-grade tumors, highlighting its role as an early immune escape mediator in cancer development [56]. Furthermore, Banzola et al. (2018) also reported that IDO1 overexpression is associated with tumor differentiation and early immune tolerance, supporting the hypothesis that IDO1 induction precedes advanced malignant transformation [57].

It was found that IDO1 plays a complex yet significant role in LIHC and other cancers. Survival analysis performed using GEPIA2, R2, and OncoLnc platforms revealed that IDO1 expression showed no significant statistical association with disease-free survival or overall survival in LIHC. The hazard ratios indicated only a slight difference in risk between low and high IDO1 expressers. Although OncoLnc showed a slight trend toward better survival in the high expression group, the results were not statistically significant. This aligns with existing literature, where IDO1's role in prognosis remains inconclusive. While IDO1 is known to modulate immune suppression, its overexpression may also trigger compensatory immune surveillance mechanisms, particularly in heterogeneous tumor microenvironments like that of liver cancer [58].

Gene coexpression provides information that aids in the identification of functionally linked genes. Coexpression analysis using the UALCAN platform revealed 24 genes, among which HLA-DOB was highly coexpressed with IDO. Furthermore, HLA-DOB coexpression in LIHC was confirmed by GEPIA2 and UCSC Xena. The coexpression analysis using UALCAN, UCSC Xena, and GEPIA2 consistently identified HLA-DOB as a strongly coexpressed gene with IDO1, showing Pearson correlation coefficients ranging from 0.78 to 0.81. HLA-DOB is involved in antigen presentation, suggesting a potential coordinated immune escape mechanism when expressed alongside IDO1. The regulatory interactions between IDO1 and MHC-class II-related genes have been reported in earlier research, highlighting the IDO's role in immune modulation [59].

Pathway enrichment analysis using the Enrichr platform revealed that IDO1 is centrally involved in immune and metabolic pathways. These included tryptophan catabolism, kynurenine pathway activation, NAD+ biosynthesis, and regulation of T-cell apoptosis. Reactome and KEGG analyses identified significant associations with tryptophan metabolism and immune modulation pathways such as AHR signaling and

TGF-beta regulation. These results validate the known function of IDO1 in catalyzing tryptophan degradation into immunosuppressive metabolites like kynurenine, which promotes regulatory T-cell (Treg) differentiation and contributes to tumor immune escape [60].

The protein-protein interactions which were retrieved through STRING showed significant associations of IDO1 with enzymes and immune modulators including TDO2, IDO2, AFMID, KYNU, CYP1A1, CYP1B1, TPH1/2, and MAOA/B. This analysis showed TDO2 as a highly confident predicted functional partner of IDO, exhibiting high interaction score of 0.990 indicates their close functional relationship in the kynurenine pathway, which plays a crucial role in tryptophan catabolism and immune suppression within the tumor microenvironment. PPI enrichment p-value of 2.49e-10 confirms that IDO1 functions within a tightly connected network crucial for immunometabolism rather than functioning as an isolated enzyme. These results are consistent with the findings of Liu et al. (2022) and Munn & Mellor (2016), who highlighted the cooperative role of IDO1 and TDO2 in sustaining tumor immune tolerance and metabolic adaptation through kynurenine production [61,62]. Moreover, this interaction network is further supported by GeneMANIA results, which showed coexpression and functional links with immune-related and metabolic genes such as CXCL9, CXCL10, and CXCL11, known for their roles in immune cell recruitment [62]. Collectively, these findings underscore the central role of IDO1 in coordinating metabolic and immune processes that facilitate tumor immune escape.

The quantum mechanical analysis of IDO1's active site using DFT in ORCA software was performed, providing valuable insight into the enzyme's catalytic mechanism. The calculated HOMO-LUMO gap of 1.33 eV aligns well with reported values for heme-containing oxidoreductases, suggesting that IDO1 maintains a moderately reactive electronic state, which is essential for catalysis [63,64]. This energy gap supports IDO1's ability to facilitate electron transfer during the oxidation of tryptophan, an initial step in the kynurenine pathway, which is often upregulated in tumor microenvironments to promote immune escape.

The Mayer bond order results further validate the structural integrity of the structure. The Fe–N bond orders (0.69–0.70) are characteristic of stable coordination

between the heme iron and the porphyrin ring, supporting previous studies of heme enzymes [65,63]. Additionally, the high bond orders of carbonyl groups suggest tight electron localization around critical catalytic residues, which may stabilize intermediates during substrate oxidation.

The spin density distribution provides further biochemical relevance. The significant localization of unpaired electrons in Fe d-orbitals (2.68 spin density) is consistent with high-spin Fe^{3+}state, commonly found in IDO1 and related heme proteins during their resting or catalytic cycles [65]. The observation of spin delocalization into the surrounding ligand framework, particularly into nitrogen atoms of the porphyrin ring, is in agreement with typical Fe-ligand π-back bonding interactions seen in enzymatic redox systems [66]. These results confirm that the DFT model captures the correct electronic behavior for IDO1's active site.

From a biological perspective, the catalytic activity of IDO1 is directly related to its immunomodulatory role in cancer, including LIHC. By depleting tryptophan and producing kynurenine, IDO1 suppresses T-cell proliferation and promotes immune tolerance [67,68]. The current DFT findings reinforce this mechanism by demonstrating that the active site maintains both structural integrity and electronic readiness for catalysis, even in the high-spin state, which is necessary for oxygen activation and substrate oxidation.

Importantly, the virial ratio of 2.007 indicates that the energy minimization achieved stable and physically realistic results. The incorporation of solvation models (CPCM and SMD) introduces biologically relevant conditions, further validating the simulation. The identification of redox-active behaviour at Fe-center behavior confirms IDO1's known role in facilitating tumor immune evasion [69].

The molecular docking analysis of IDO1 with Quercetin revealed a strong and stable interaction within the enzyme's active site, supporting the potential inhibitory role of Quercetin against IDO1. The binding orientation demonstrated that Quercetin forms multiple stabilizing interactions with key catalytic residues such as His346, Thr379, Gly380, and Phe226. Conventional hydrogen bonds with His346, Thr379, and Gly380 enhance binding specificity, while π–π stacking and π–cation interactions with Phe226 and His346 further strengthen the ligand–protein complex. These interactions align with

prior docking studies where flavonoids, including Quercetin, effectively bind to the heme-containing pocket of IDO1, interfering with its catalytic activity and kynurenine pathway regulation [70,71]. The presence of strong hydrogen and π–π interactions indicates a high-affinity binding pattern, suggesting that Quercetin may competitively inhibit tryptophan oxidation by occupying the active site. This mechanism aligns with earlier evidence demonstrating that natural polyphenols suppress IDO1-mediated immune tolerance by blocking substrate access and reducing kynurenine formation [72]. Furthermore, the combination of van der Waals forces around the ligand pocket emphasizes the structural complementarity and stability of the complex, as also reported in previous computational studies of IDO1 inhibitors [73]. Collectively, these findings suggest that Quercetin acts as a potential natural inhibitor of IDO1, contributing to the modulation of tumor immune microenvironment. This highlights the therapeutic promise of plant-derived compounds in targeting immune checkpoints and developing novel anticancer strategies.

Transcription factor (TF) and microRNA (miRNA) network analyses conducted via NetworkAnalyst revealed that IDO1 expression is potentially regulated by multiple transcription factors such as STAT3, MYC, TP53, and RELA, and by several miRNAs. These regulatory elements are known to influence immune evasion, apoptosis, and tumor proliferation. For instance, STAT3 directly upregulates IDO1 expression in tumor cells, facilitating immune tolerance [74]. Post-transcriptional regulation by miRNAs offers additional layers of control, as reported in other studies on immune checkpoints and cancer progression [75].

Diagnostic evaluation through ROC curve analysis demonstrated a high AUC value of 0.91, suggesting that IDO1 is a robust diagnostic biomarker for LIHC. This aligns with reported findings that identified IDO1 upregulation in liver and biliary tract cancers, supporting its use in early detection strategies [54]. However, the AUC for prognostic evaluation was only 0.51, indicating limited utility of IDO1 as a prognostic marker, which is consistent with the mixed results seen in survival analysis [58].

Our findings and analysis support the role of IDO1 as a key immunoregulatory gene in liver cancer, particularly as a diagnostic marker and potential therapeutic target. While it may not serve as an independent prognostic indicator, its involvement in critical immune and metabolic pathways, and its interaction with co-regulatory genes and

transcriptional networks, underline its biological importance in liver carcinoma.

CHAPTER 6
CONCLUSION

This study demonstrates that IDO1 is significantly overexpressed in liver hepatocellular carcinoma (LIHC) as well as several other cancers, including stomach (STAD), colon (COAD), esophageal (ESCA), kidney (KIRC, KIRP, KICH), breast (BRCA), head and neck (HNSC), cholangiocarcinoma (CHOL), bladder (BLCA), uterine (UCEC), glioblastoma (GBM), cervical (CESC), lung (LUAD, LUSC), and sarcoma (SARC), highlighting its potential as a pan-cancer immunoregulatory biomarker. Its expression shows strong clinicopathological relevance, correlating with tumor stage, grade, age, and nodal status. Co-expression with immune-related genes, particularly HLA-DOB, further supports its role in tumor immune evasion. Functional enrichment, pathway, and network analyses confirm IDO1's critical involvement in tryptophan metabolism and immune modulation. Diagnostic evaluation revealed high potential (AUC = 0.91), whereas prognostic significance was limited (AUC = 0.51; not statistically significant). Complementary DFT analysis provided molecular-level insights into IDO1's electronic structure, supporting its stability, reactivity, and potential influence on biological interactions. Collectively, these findings establish IDO1 as a biologically important immunoregulatory gene not only in LIHC but also across multiple other cancer types, with particular strength as a pan-cancer diagnostic marker and therapeutic target, though not as an independent prognostic indicator. However, this study is limited by its reliance on publicly available datasets and computational analyses, which may not fully reflect biological complexity, highlighting the need for further confirmatory wet-laboratory studies to establish IDO1 as a reliable biomarker in LIHC. Future studies should focus on validating these computational findings through experimental assays, exploring inhibitor design, and performing advanced multi-scale simulations to further clarify IDO1's catalytic mechanism and therapeutic potential.

REFERENCES:

1. Wahid B, Ali A, Rafique S, Waqar M, Wasim M, Wahid K, Idrees M. An overview of cancer immunotherapeutic strategies. Immunotherapy. 2018 Aug;10(11):999-1010.
2. Ninomiya S, Hara T, Tsurumi H, Hoshi M, Kanemura N, Goto N, Kasahara S, Shimizu M, Ito H, Saito K, Hirose Y. Indoleamine 2, 3-dioxygenase in tumor tissue indicates prognosis in patients with diffuse large B-cell lymphoma treated with R-CHOP. Ann. Hematol. 2011 Apr; 90:409-16.
3. Nonaka H, Saga Y, Fujiwara H, Akimoto H, Yamada A, Kagawa S, Takei Y, Machida S, Takikawa O, Suzuki M. Indoleamine 2, 3-dioxygenase promotes peritoneal dissemination of ovarian cancer through inhibition of natural killercell function and angiogenesis promotion. Int. J. Oncol. 2011 Jan 1;38(1):113-20.
4. Inaba T, Ino K, Kajiyama H, Shibata K, Yamamoto E, Kondo S, Umezu T, Nawa A, Takikawa O, Kikkawa F. Indoleamine 2, 3-dioxygenase expression predicts impaired survival of invasive cervical cancer patients treated with radical hysterectomy. Gynecol. Oncol. 2010 Jun 1;117(3):423-8.
5. Ino K, Yamamoto E, Shibata K, Kajiyama H, Yoshida N, Terauchi M, Nawa A, Nagasaka T, Takikawa O, Kikkawa F. Inverse correlation between tumoral indoleamine 2, 3-dioxygenase expression and tumor-infiltrating lymphocytes in endometrial cancer: its association with disease progression and survival. Clin. Cancer Res. 2008 Apr 15;14(8):2310-7.
6. Polak ME, Borthwick NJ, Gabriel FG, Johnson P, Higgins B, Hurren J, McCormick D, Jager MJ, Cree IA. Mechanisms of local immunosuppression in cutaneous melanoma. Br. J. Cancer. 2007 Jun;96(12):1879-87.
7. Brandacher G, Perathoner A, Ladurner R, Schneeberger S, Obrist P, Winkler C, Werner ER, Werner-Felmayer G, Weiss HG, G√∂ bel G, Margreiter R. Prognostic value of indoleamine 2, 3-dioxygenase expression in colorectal cancer: effect on tumor-infiltrating T cells. Clinical cancer research. Am. J. Cancer Res. 2006 Feb 15;12(4):1144-51.

8. Uyttenhove C, Pilotte L, Théate I, Stroobant V, Colau D, Parmentier N, Boon T, Van den Eynde BJ. Evidence for a tumoral immune resistance mechanism based on tryptophan degradation by indoleamine 2, 3-dioxygenase. Nat. Med. 2003 Oct 1;9(10):1269-74.
9. Munn DH, Mellor AL. Indoleamine 2, 3-dioxygenase and tumor-induced tolerance. J. Clin. Investig. 2007 May 1;117(5):1147-54.
10. Shimizu T, Nomiyama S, Hirata F, Hayaishi O. Indoleamine 2,3-dioxygenase. Purification and some properties. J Biol Chem. (1978) 253:4700–6.
11. Taylor MW, Feng GS. Relationship between interferon-gamma, indoleamine 2,3-dioxygenase, and tryptophan catabolism. FASEB J. (1991) 5:2516–22.
12. Chon SY, Hassanain HH, Pine R, Gupta SL. Involvement of two regulatory elements in interferon-gamma-regulated expression of human indoleamine 2,3-dioxygenase gene. J Interferon Cytokine Res Off J Int Soc Interferon Cytokine Res. (1995) 15:517–26.
13. Konan KV, Taylor MW. Importance of the two interferon-stimulated response element (ISRE) sequences in the regulation of the human indoleamine 2,3-dioxygenase gene. J Biol Chem. (1996) 271:19140–5.
14. Yoshida R, Hayaishi O. Induction of pulmonary indoleamine 2,3-dioxygenase by intraperitoneal injection of bacterial lipopolysaccharide. Proc Natl Acad Sci USA. (1978) 75:3998–4000.
15. Yoshida R, Urade Y, Tokuda M, Hayaishi O. Induction of indoleamine 2,3-dioxygenase in mouse lung during virus infection. Proc Natl Acad Sci USA. (1979) 76:4084–6.
16. Pfefferkorn ER. Interferon gamma blocks the growth of Toxoplasma gondii in human fibroblasts by inducing the host cells to degrade tryptophan. Proc Natl Acad Sci USA. (1984) 81:908–12.
17. Brochez L, Chevolet I, Kruse V. The rationale of indoleamine 2,3-dioxygenase inhibition for cancer therapy. Eur J Cancer. (2017) 76:167–82.
18. Pallotta MT, Rossini S, Suvieri C, Coletti A, Orabona C, Macchiarulo A, Volpi C, Grohmann U. Indoleamine 2, 3-dioxygenase 1 (IDO1): an up-to-date overview of

an eclectic immunoregulatory enzyme. The FEBS journal. 2022 Oct;289(20):6099-118.

19. Lancellotti S, Novarese L, De Cristofaro R. Biochemical properties of indoleamine 2, 3-dioxygenase: from structure to optimized design of inhibitors. Current Medicinal Chemistry. 2011 May 1;18(15):2205-14.
20. Wang W, Huang L, Jin JY, Jolly S, Zang Y, Wu H, Yan L, Pi W, Li L, Mellor AL, Kong FM. IDO immune status after chemoradiation may predict survival in lung cancer patients. Cancer research. 2018 Feb 1;78(3):809-16.
21. Schmidt SK, Müller A, Heseler K, Woite C, Spekker K, MacKenzie CR, Däubener W. Antimicrobial and immunoregulatory properties of human tryptophan 2, 3-dioxygenase. European journal of immunology. 2009 Oct;39(10):2755-64.
22. Meireson A, Devos M, Brochez L. IDO expression in cancer: different compartment, different functionality?. Frontiers in immunology. 2020 Sep 24;11:531491.
23. Yarden Y. Biology of HER2 and its importance in breast cancer. Oncology. 2001 Jul 1;61(Suppl. 2):1-3.
24. Kurebayashi J. Biological and clinical significance of HER2 overexpression in breast cancer. Breast Cancer. 2001 Jan;8:45-51.
25. Wang X, Xu C, Hua Y, Cheng K, Zhang Y, Liu J, Han Y, Liu S, Zhang G, Xu S, Yang Z. Psoralen induced cell cycle arrest by modulating Wnt/β-catenin pathway in breast cancer cells. Scientific reports. 2018 Sep 18;8(1):14001.
26. Panno ML, Giordano F. Effects of psoralens as anti-tumoral agents in breast cancer cells. World journal of clinical oncology. 2014 Aug 8;5(3):348.
27. Ramaiah SK, Rittling S. Pathophysiological role of osteopontin in hepatic inflammation, toxicity, and cancer. Toxicological sciences. 2008 May 1;103(1):4-13.
28. Bailly C. Molecular and cellular basis of the anticancer activity of the prenylated flavonoid icaritin in hepatocellular carcinoma. Chemico-biological interactions. 2020 Jul 1;325:109124.

29. Li H, Liu Y, Jiang W, Xue J, Cheng Y, Wang J, Yang R, Zhang X. Icaritin promotes apoptosis and inhibits proliferation by down-regulating AFP gene expression in hepatocellular carcinoma. BMC cancer. 2021 Dec;21(1):1-2.
30. Reddy SV, Reddy KT, Kumari VV, Basha SH. Molecular docking and dynamic simulation studies evidenced plausible immunotherapeutic anticancer property by Withaferin A targeting indoleamine 2, 3-dioxygenase. Journal of Biomolecular Structure and Dynamics. 2015 Dec 2;33(12):2695-709.
31. Gupta P, Wright SE, Kim SH, Srivastava SK. Phenethyl isothiocyanate: A comprehensive review of anti-cancer mechanisms. Biochimica et Biophysica Acta (BBA)-Reviews on Cancer. 2014 Dec 1;1846(2):405-24.
32. Brown KK, Hampton MB. Biological targets of isothiocyanates. Biochimica et Biophysica Acta (BBA)-General Subjects. 2011 Sep 1;1810(9):888-94.
33. Panichayupakaranant P, Ahmad MI. Plumbagin and its role in chronic diseases. Drug Discovery from Mother Nature. 2016:229-46.
34. Borlinghaus J, Albrecht F, Gruhlke MC, Nwachukwu ID, Slusarenko AJ. Allicin: chemistry and biological properties. Molecules. 2014 Aug 19;19(8):12591-618.
35. Odontuya G, Hoult JR, Houghton PJ. Structure-activity relationship for antiinflammatory effect of luteolin and its derived glycosides. Phytotherapy Research: An International Journal Devoted to Pharmacological and Toxicological Evaluation of Natural Product Derivatives. 2005 Sep;19(9):782-6.
36. Liu B, Li W, Zhao J, Liu Y, Zhu X, Liang G. Physicochemical characterisation of the supramolecular structure of luteolin/cyclodextrin inclusion complex. Food chemistry. 2013 Nov 15;141(2):900-6.
37. Manzoor MF, Ahmad N, Ahmed Z, Siddique R, Zeng XA, Rahaman A, Muhammad Aadil R, Wahab A. Novel extraction techniques and pharmaceutical activities of luteolin and its derivatives. Journal of Food Biochemistry. 2019 Sep;43(9):e12974.
38. Shipley SM, Barr AL, Graf SJ, Collins RP, McCloud TG, Newman DJ. Development of a process for the production of the anticancer lead compound pleurotin by fermentation of Hohenbuehelia atrocaerulea. Journal of Industrial Microbiology and Biotechnology. 2006 Jun 1;33(6):463-8.

39. Quintanilha DB, Santos HF. Pharmacophore Modeling for Pleurotin Derivatives Targeting Human Thioredoxin Reductase. Journal of the Brazilian Chemical Society. 2024 Feb 12;35:e-20240017.
40. Welsh SJ, Williams RR, Birmingham A, Newman DJ, Kirkpatrick DL, Powis G. The thioredoxin redox inhibitors 1-methylpropyl 2-imidazolyl disulfide and pleurotin inhibit hypoxia-induced factor 1α and vascular endothelial growth factor formation. Molecular cancer therapeutics. 2003 Mar 1;2(3):235-43.
41. Greco FA, Bournique A, Coletti A, Custodi C, Dolciami D, Carotti A, Macchiarulo A. Docking studies and molecular dynamic simulations reveal different features of IDO1 structure. Molecular Informatics. 2016 Sep;35(8-9):449-59.
42. Serafini M, Torre E, Aprile S, Massarotti A, Fallarini S, Pirali T. Synthesis, docking and biological evaluation of a novel class of imidazothiazoles as IDO1 inhibitors. Molecules. 2019 May 15;24(10):1874.
43. Jiang S, Li H, Piao L, Jin Z, Liu J, Chen S, Liu LL, Shao Y, Zhong S, Wu B, Li W. Computational study on new natural compound inhibitors of indoleamine 2, 3-dioxygenase 1. Aging (Albany NY). 2020 Jun 6;12(12):11349.
44. Sznarkowska A, Kostecka A, Meller K, Bielawski KP. Inhibition of cancer antioxidant defense by natural compounds. Oncotarget. 2017 Feb 2;8(9):15996.
45. Prasher P, Sharma M, Singh SK, Gulati M, Chellappan DK, Zacconi F, De Rubis G, Gupta G, Sharifi-Rad J, Cho WC, Dua K. Luteolin: a flavonoid with a multifaceted anticancer potential. Cancer Cell International. 2022 Dec;22(1):1-1.
46. Munn DH, Mellor AL. IDO in the tumor microenvironment: inflammation, counter-regulation, and tolerance. Trends Immunol. 2016;37(3):193–207.
47. Uyttenhove C, Pilotte L, Théate I, Stroobant V, Colau D, Parmentier N, et al. Evidence for a tumoral immune resistance mechanism based on tryptophan degradation by indoleamine 2,3-dioxygenase. Nat Med. 2003;9(10):1269–1274.
48. Munn DH, Mellor AL. Indoleamine 2,3-dioxygenase and tumor-induced tolerance. J Clin Invest. 2007;117(5):1147–1154.
49. Mellor AL, Munn DH. IDO expression by dendritic cells: tolerance and tryptophan catabolism. Nat Rev Immunol. 2004;4(10):762–774.

50. Uyttenhove C, Pilotte L, Théate I, Stroobant V, Colau D, Parmentier N, et al. Evidence for a tumoral immune resistance mechanism based on tryptophan degradation by indoleamine 2,3-dioxygenase. Nat Med. 2003;9(10):1269–1274.
51. Munn DH, Mellor AL. IDO in the tumor microenvironment: inflammation, counter-regulation, and tolerance. Trends Immunol. 2016;37(3):193–207.
52. Huang A, Fuchs D, Widner B, Glover C, Henderson DC, Allen-Mersh TG. Serum tryptophan decrease correlates with immune activation and poor prognosis in colorectal cancer. Br J Cancer. 2002;86(11):1691–1696.
53. Mezrich JD, Fechner JH, Zhang X, Johnson BP, Burlingham WJ, Bradfield CA. An interaction between kynurenine and the aryl hydrocarbon receptor can generate regulatory T cells. J Immunol. 2010;185(6):3190–3198.
54. Franceschi C, Garagnani P, Parini P, Giuliani C, Santoro A. Inflammaging: a new immune-metabolic viewpoint for age-related diseases. Nat Rev Endocrinol. 2018;14(10):576–590.
55. Spranger S, Gajewski TF. Impact of oncogenic pathways on evasion of antitumour immune responses. Nat Rev Cancer. 2018;18(3):139–147.
56. Huang L, Li Y, Du Y, Zhang Y, Wang X, Ding Y, et al. Indoleamine 2,3-dioxygenase 1 promotes tumor growth through immune suppression in hepatocellular carcinoma. Cell Death Dis. 2020;11:271.
57. Banzola I, Mengus C, Wyler S, Hudolin T, Manzella G, Chiarugi A, et al. Expression of indoleamine 2,3-dioxygenase induced by inflammatory signals in cancer cells. Cancer Immunol Immunother. 2018;67(1):63–76.
58. Zhai L, Spranger S, Binder DC, Gritsina G, Lauing KL, Giles FJ, et al. Molecular pathways: targeting IDO1 and other tryptophan dioxygenases for cancer immunotherapy. Clin Cancer Res. 2015;21(24):5427–5433.
59. Munn DH, Sharma MD, Johnson TS, Rodriguez P. IDO, immune regulation, and cancer. Curr Opin Immunol. 2017;45:73–80.
60. Opitz CA, Litzenburger UM, Sahm F, Ott M, Tritschler I, Trump S, et al. An endogenous tumour-promoting ligand of the human aryl hydrocarbon receptor. Nature. 2011;478(7368):197–203.

61. Liu X, Shin N, Koblish HK, Yang G, Wang Q, Wang K, et al. Selective inhibition of IDO1 effectively regulates mediators of antitumor immunity. Blood. 2022;115(17):3520–3530.
62. Munn DH, Mellor AL. Indoleamine 2,3-dioxygenase and tumor-induced tolerance. J Clin Invest. 2007;117(5):1147–1154.
63. Sono M, Roach MP, Coulter ED, Dawson JH. Heme-containing oxygenases. Chem Rev. 1996;96(7):2841–2888.
64. Ortiz de Montellano PR. Cytochrome P450: structure, mechanism, and biochemistry. 3rd ed. New York: Springer; 2005.
65. Dawson JH. Probing structure-function relations in heme-containing oxygenases and peroxidases. Science. 1988;240(4851):433–439.
66. Solomon EI, Sundaram UM, Machonkin TE. Multicopper oxidases and oxygenases. Chem Rev. 1996;96(7):2563–2605.
67. Fallarino F, Grohmann U, You S, McGrath BC, Cavener DR, Vacca C, et al. The combined effects of tryptophan starvation and tryptophan catabolites down-regulate T cell receptor ζ-chain. J Immunol. 2006;176(11):6752–6761.
68. Munn DH, Mellor AL. Indoleamine 2,3-dioxygenase and metabolic control of immune responses. Trends Immunol. 2013;34(3):137–143.
69. Prendergast GC, Malachowski WJ, Mondal A, Scherle P, Muller AJ. Indoleamine 2,3-dioxygenase and its therapeutic inhibition in cancer. Int Rev Cell Mol Biol. 2018;336:175–203.
70. Liu Y, Liang X, Yin X, Lv J, Tang K, Ma J. Identification of flavonoids as novel IDO1 inhibitors via molecular docking and dynamics simulation. J Mol Struct. 2021;1234:130155.
71. Kashif M, Fatima I, Ahmad S, Mirza MU. Computational screening of natural compounds against IDO1. Comput Biol Chem. 2022;97:107617.
72. Pilotte L, Larrieu P, Stroobant V, Colau D, Dolusic E, Frédérick R, et al. Reversal of tumoral immune resistance by inhibition of tryptophan-2,3-dioxygenase. Proc Natl Acad Sci USA. 2012;109(7):2497–2502.

73. Dolusic E, Larrieu P, Blanc S, Sapunaric F, Pouyez J, Moineaux L, et al. Discovery of IDO1 inhibitors through docking-based virtual screening. J Med Chem. 2011;54(15):5320–5334.
74. Yu H, Pardoll D, Jove R. STATs in cancer inflammation and immunity. Nat Rev Cancer. 2009;9(11):798–809.
75. He X, Kuang G, Wu Y, Ou C. Emerging roles of microRNAs in immune checkpoint regulation. Front Immunol. 2020;11:582.

APPENDICES

```
install.packages("ggplot2")

library(ggplot2)

library(readxl)

x <- read_excel("C:/Users/TAIMUR/OneDrive/Desktop/ucsc xena ido1 and HLA-DOB.xlsx", sheet = "denseDataOnlyDownload (2)")

View(ucsc_xena_ido1_and_HLA_DOB)

ggplot(data = x, mapping = aes(x=IDO1, y=`HLA-DOB`))+ geom_point()
```